

# Near-Field Electrospinning: Progress and Applications

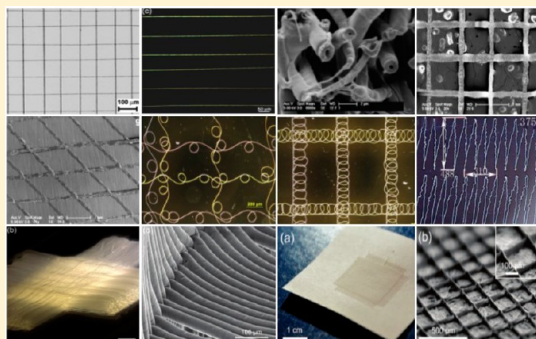
Xiao-Xiao He,<sup>†,⊥</sup> Jie Zheng,<sup>‡,⊥</sup> Gui-Feng Yu,<sup>†</sup> Ming-Hao You,<sup>†</sup> Miao Yu,<sup>†,§</sup> Xin Ning,<sup>‡</sup> and Yun-Ze Long<sup>\*,†,‡,⊥</sup>

<sup>†</sup>Collaborative Innovation Center for Nanomaterials & Devices, College of Physics, Qingdao University, Qingdao 266071, China

<sup>‡</sup>Industrial Research Institute of Nonwovens & Technical Textiles, College of Textiles & Clothing, Qingdao University, Qingdao 266071, China

<sup>§</sup>Department of Mechanical Engineering, Columbia University, New York, New York 10027, United States

**ABSTRACT:** Electrospinning is a straightforward and versatile method to fabricate ultrafine fibers with unique physical and chemical properties. However, the chaotic nature of traditional electrospinning limits its applications in devices which usually need arranged or patterned micro/nanoscale fibrous structures. In order to improve the controllable deposition of electrospun fibers, near-field electrospinning (NFES) has been proposed and developed in recent years. With characteristics of position-controlled deposition, NFES significantly expands the range of fiber-fabrication uses including electronic components, energy harvesting, flexible sensors, and tissue engineering. In this paper, the basic principle and research advances of NFES have been briefly reviewed. In particular, we summarize the process parameters, polymer materials, as-spun fibrous structures, modified apparatus, and potential applications of NFES. Finally, future prospects on the development tendency and challenges of NFES are discussed.



## 1. INTRODUCTION

Owing to the superior advantages of small diameter,<sup>1,2</sup> fascinating flexibility,<sup>3,4</sup> and other unique physical and chemical properties, one-dimensional (1D) nanostructures have been synthesized as building blocks to distinctly enhance the performance of various advanced functional devices.<sup>5–9</sup> Although there are numerous approaches to fabricate nanofibers,<sup>10</sup> electrospinning becomes more attractive due to its well-known simplicity, extensive applicability, and high efficiency. Not only polymers but also inorganic materials<sup>11–13</sup> can be electrospun. And, as is known to the scientific community, the two fundamental forms of electrospinning are solution electrospinning (SES) and melt electrospinning (MES) (or solvent-free electrospinning).<sup>14–17</sup> In spite of the wider field of feasibility, conventional SES is facing the challenges of environmental pollution, health threats, and low productivity caused by solvent evaporation. On the contrary, as an eco-friendly nanofiber fabricating approach, MES successfully avoids the evaporation of solvent, and it provides great opportunities in biomedical engineering, but it requires a higher spinning temperature and more complex apparatus.<sup>18–21</sup> In short, both of the two forms have their own pros and cons. Moreover, the nonwoven fibrous films (deposited in random orientation) prepared by the two forms of traditional electrospinning (TES) restrict the potential applications in some precise fabrication fields, such as electronic components, flexible devices, and bioengineering.

To improve the controllability of fiber deposition and fiber structure, TES has been modified by a large margin to meet the specific requirement. Previous improvements are mostly

concentrated on spinning nozzle and collector.<sup>3,22–25</sup> In recent years, low-voltage electrospinning has been proposed and developed. At present, three main patterns are reported to realize low-voltage electrospinning: the first is to increase the auxiliary forces to reduce the electric field force;<sup>26</sup> the second is to change the dope composition via adding appropriate characteristic materials;<sup>27</sup> the third is to decrease the spinning distance. In the above three methods, the most effective one is to decrease the spinning distance, namely near-field electrospinning (NFES).<sup>28</sup> NFES not only reduces spinning voltage but also achieves the aim of controllable precision deposition of fibers. This effect opens an interesting perspective for the realization of position-controlled deposition and precise integration of individual or aligned fibers with flexible and functional devices, which greatly expands its application fields ranging over nanogenerator, tissue engineering, wearable sensors, nanodevices, microelectromechanical systems (MEMS),<sup>29–40</sup> etc.

The purpose of NFES is to realize controllable deposition and low-voltage electrospinning. For the TES process, under the action of electric field, the charged jet flows away from the charged drop and moves along a nearly straight line in the initial stage. Then as the stretching and thinning take place, it turns into bending instability because of the repulsive forces originated from the charged elements in the jet. Finally, helical or wavy fibers are deposited randomly on the collector due to the chaotic

**Received:** December 20, 2016

**Revised:** March 7, 2017

**Published:** March 7, 2017

Table 1. Comparison between TES and NFES

| method | forms                    | distance (cm) | voltage (kV) | collector      | fiber diameter ( $\mu\text{m}$ ) | advantages  | disadvantages   |
|--------|--------------------------|---------------|--------------|----------------|----------------------------------|---|---|
| TES    | SES; MES                 | 5–50          | 10–30        | static/dynamic | 0.01–1                           | *simple device<br>*large-scale fabrication<br>*various applicable materials | *random deposition<br>*high voltage                                   |
| NFES   | solution NFES; melt NFES | 0.05–5        | 0.2–12       | static/dynamic | 0.05–30                          | *controllable deposition<br>*low voltage<br>*precise fabrication            | *immature mechanism<br>*larger diameter<br>*smaller-scale fabrication |

Table 2. Effects of NFES Parameters on Fiber Diameter and Morphology

| parameter varied   | parameters kept constant                               | key observations                                       | references |
|--|--|--|------------|
| spinning voltage (V) 200 $\rightarrow$ 600                       | 2 wt % PEO, $D = 1$ mm, CMS = 0.04 m/s                 | fiber diameter increases with increasing voltage       | 47         |
| CMS (m/s) 0.02 $\rightarrow$ 0.08                                | 2 wt % PEO, $D = 1$ mm, $V = 400$ V                    | fiber diameter decreases with increasing CMS           |            |
| spinning distance ( $D$ , $\mu\text{m}$ ) 500 $\rightarrow$ 1500 | 7 wt % PEO, $V = 800$ V, CMS = 0.12 m/s                | fiber diameter decreases with increasing distance      | 46         |
| polymer concentration PEO: 3 wt % $\rightarrow$ 9 wt %           | $D = 1000$ $\mu\text{m}$ , $V = 500$ V, CMS = 0.12 m/s | fiber diameter increases with increasing concentration |            |
| CMS (m/s) > 0.35 $\rightarrow$ 0.05                              | 20 wt % PEO, $D = 1$ mm, $V = 1.7$ kV                  | fiber shaped in straight line                          | 44         |
|  | 0.15 $\rightarrow$ 0.35                                | fiber shaped in waved line                             |            |
|  | 0.08 $\rightarrow$ 0.15                                | fiber shaped in single circle coil                     |            |
|  | < 0.08   | fiber shaped in multi circle coil                      |            |

motion.<sup>41–43</sup> So the nanofibers produced by TES are usually in a form of disordered nonwoven film. In the NFES approach, the bending instability can be significantly restricted due to the shorter spinning distance, so the fibers can be deposited with a good controllability in straight-line stage. Meanwhile, the collector is put on a two-dimensional (2D) motion platform which is controlled by computer program exactly, so the fibers with predesigned trajectories can be deposited. By changing the collector moving speed (CMS), coiled, waved and straight-line nanofiber can be obtained successively, as the effect of residual charges on collector is weakened by the strong drag force from the fast moving.<sup>44,45</sup> And similarly, NFES also contains two fundamental forms of solution NFES and melt NFES. Table 1 shows the comparison between TES and NFES.

Although NFES can reduce spinning voltage effectively and deposit fibers accurately, the limitation of polymer solution dipped by probe tip restricts the continuous large-scale preparation of fibers;<sup>28</sup> furthermore, the shortened distance between spinneret and collecting plate limits the stretching and thinning of fibers, which tends to increase fiber diameters.<sup>46</sup> They are the main suppression factors of NFES in the initial stage. Fortunately, as the deepening of the research about NFES takes place, these problems have been solved step by step. To be sure, the establishment of NFES and its relevant techniques have largely strengthened the controllability of fibrous structure, internal crystallizing,<sup>35</sup> and integration with devices. Relevant researches show that the fiber diameters and morphologies can be influenced by solution concentration, spinning voltage, spinning distance, and the matched degree of CMS and electrospinning speed;<sup>44,46–49</sup> examples are shown in Table 2. Besides, other factors like the spinneret diameter, the surface tension, the electrical charge, and the humidity will also influence the deposition behavior of NFES fibers, which need to be further researched.<sup>28,44,50</sup>

In this review, we briefly summarized the recent research advances in NFES mainly including process conditions, electrospun fibers, and their corresponding applications. Other items regarding the mechanism, the superiority, and some limitations, as well as the development tendency, have also been discussed in the paper. These encouraging achievements have demonstrated that NFES is a promising technique with combination of

controllable fiber deposition, which may open up a new prospect for the expansive fabrication and integration of micro/nanofibers in various applications.

## 2. PROGRESS AND MECHANISM OF NFES

1D nanotubes, nanowires, and nanofibers have been extensively developed in recent years as potential fundamental elements for micro-/nanoscale electronics, biological/chemical sensing, energy harvesting and tissue engineering. Many fabrication methods have been invested, such as solution growth, chemical vapor deposition, lithography technologies, contact or roll printing, template-guided synthesis, and electrospinning. However, most of the approaches usually have random orientation and alignment for 1D nanostructures, and some of them are complicated and sophisticated. As a kind of emerging electrospinning technique, NFES has been used in many applications. In NFES progress, the bending instability is significantly restricted due to the decreasing of spinning distance, so fibers can be deposited with controllability in straight-line stage. NFES realizes position-controlled deposition in predesigned trajectory and the construction of aligned fibers and 3D fibrous structures. Meanwhile, NFES needs no elaborate template and postprocessing, which is a convenient and low-cost fiber preparation technique. In this section, we briefly introduce the progress and mechanism of NFES.

**2.1. Development of NFES.** The TES system has been mostly used in the fabrication of randomly deposited polymeric fibers.<sup>3,5,6</sup> However, it is of great interest to fabricate well-controlled nanofibers in some advanced and sophisticated system.<sup>51</sup> Lots of literatures have reported or reviewed the TES in details, here we focus on the NFES. In 2003, a technique of using scanning tip as electrospinning source to deposit oriented nanofibers was reported by Kameoka et al.<sup>52</sup> In the process, a homemade microfabricated silicon tip (gold was deposited on the surface to increase conductivity) was utilized to dip polymer solution, the deposition distance were set from 0.5 to 1 cm, the corresponding voltage was only 4–6 kV, and the orientation of the fibers were controlled by an optical chopper motor. To take the poly(ethylene oxide) (PEO) spinning precursor solution as an example, the affected parameters on

nanofiber diameters like polymer concentration and deposition distance were demonstrated. Besides, oriented latex fluorescent fibers and conductive polymeric fibers were also electrospun by this scanning tip electrospinning. Because of no need for a spinning nozzle, the required volume for the deposition is diminutive and the operation is rapid and simple; thus, this scanned electrospinning deposition system is capable to quick deposition for numerous materials. The shortcomings are that the small quantity of the dipped solution limits large-scale electrospinning and the controllability remains to be improved by utilizing electrostatic focusing. Generally, the scanning-tip electrospinning approach laid a good foundation for the rise of NFES technique.

The concept of near-field electrospinning was formally presented by Sun et al. for the first time in 2006.<sup>28</sup> In their experiments, a homemade tungsten tip with diameter of 25  $\mu\text{m}$  was utilized to dip liquid polymer solution to initiate the electrospinning, and the fibers can be deposited in a direct, continuous, and controllable manner under the control of an  $x$ - $y$  stage (Figure 1). This paper mainly studied the preparation of

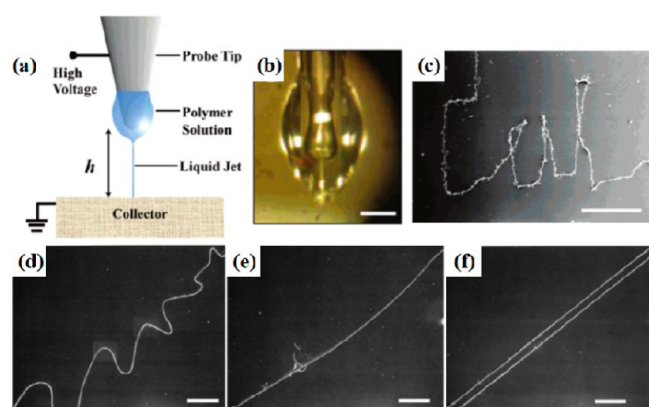


**Figure 1.** (a) Schematic illustration of NFES; (b) optical image of a polymer solution droplet attached on a tungsten electrode tip; (c–f) direct-write nanofibers with different morphologies by NFES. Reproduced from ref 28. Copyright 2006 American Chemical Society.

direct-write nanofibers. When the electrode-to-collector distance was 500  $\mu\text{m}$ , the spinning voltage could be decreased to 600 V. Different morphologies of fibers were directly written by controlling the speed and trajectory of the  $x$ - $y$  stage. Furthermore, an electrostatic field simulation for silicon substrate with or without a 2  $\mu\text{m}$  oxide-coated insulating layer was performed, and the result showed that there was no significant difference in either case under the same applied bias. Meanwhile, it had also been demonstrated that the diameters of nanofibers deposited on oxide-coated collector (50–200 nm) were usually smaller than those on silicon collector (150–300 nm). This NFES technique provides a simple, powerful and low-cost method for the controllable deposition of nanofibers, which opens a new era for the preparation of predesigned nanofibers. However, it is still limited by the droplet and cannot be used in continuous large-scale preparation, and some effect factors including the ambient parameters, the polymer solutions (surface tension, viscosity, and conductivity), and the tip diameter of the spinneret remains to be investigated systematically.

On the basis of the above two reports, NFES is gradually becoming an important branch of electrospinning. The basic principle of NFES is to realize controllable deposition by decreasing spinning distance, which could be used in fabricating

special aligned and structured fibers. More and more relevant works have been reported in recent years; the next section will introduce several representative works in detail.

**2.2. Further Research.** In order to study the deposition behavior of a single NFES nanofiber, a high-speed camera was used to reveal the formation and motion process of a charged jet. Concomitantly, a mechanism analysis was carried out to indicate the fiber deposition on preproduced substrate.<sup>45</sup> Study shows that the bending instability can be significantly overcome due to the shorter spinning distance in NFES, so the orderly direct-write nanofibers can be deposited from a straight-line jet. Via increasing collector moving speed, straight-line nanofiber can be obtained, for the effect of residual charges on collector is weakened by the strong drag force from the moving collector.

Beyond that, a comparable approach of an atomic force microscope (AFM)-based voltage-assisted electrospinning was proposed by Wu et al.<sup>53</sup> They demonstrated a feasibility of assembling single nanofiber at predetermined positions in a controllable fashion. Details for this process are illustrated in Figure 2. The applied voltage could be decreased to 8 V when the

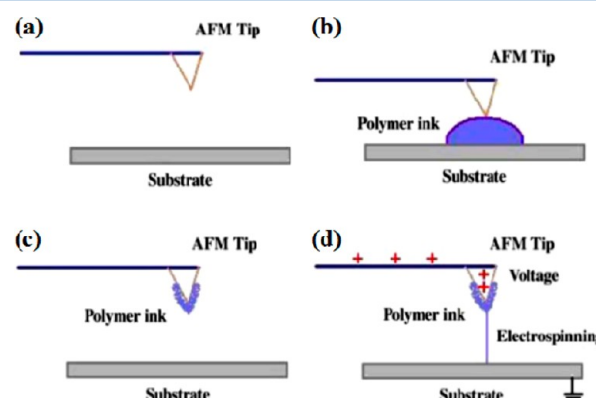


**Figure 2.** Schematic illustration of AFM-based voltage assisted electrospinning. Reproduced with permission from ref 53. Copyright 2007 Elsevier B.V.

spinning distance was set at 10  $\mu\text{m}$ , and experimental results proved that the morphology of fibers was mainly influenced by electric field intensity for this AFM-based voltage-assisted electrospinning.

According to the reported papers mentioned above, some features including the total length of nanofibers, the scale of deposition and the uniformity of thickness are limited by the polymer droplet approach for reinking the probe tip in those NFES processes. Simultaneously, the other view is that the typical probe tip is expensive and complicated for fabrication and operation. Herein, a continuous NFES to produce orderly patterned nanofibers over large areas was proposed.<sup>46</sup> Critical amelioration was showed on the spinneret and the initial mechanical drawing process (Figure 3a). First, they applied a syringe needle as spinneret to continuously supply polymer solution just as same as the TES process, then in order to electrospin sub-100 nm nanofibers, a tungsten probe tip (with tip diameter of 1  $\mu\text{m}$ ) at a voltage of 600 V was utilized to poke inside the meniscus to initial the ejection of a polymer jet by means of mechanical drawing. In this case, nanofiber with total length of 108 m was deposited in a period of 15 min, which indicated that the spinning process would keep running as long as the polymer solution was continuously supplied from the spinneret. Besides, the continuity and controllability of this



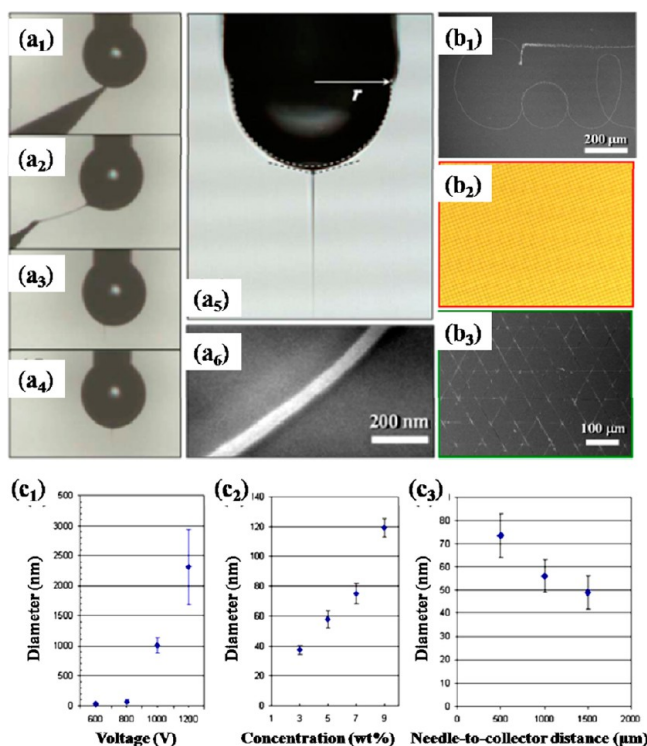


**Figure 3.** (a) Initial mechanical drawing process: (a<sub>1</sub>) A tungsten probe tip poking inside the polymer meniscus; (a<sub>2</sub>) a fiber from polymer droplet by mechanical drawing; (a<sub>3</sub>) the initiated electrospinning process; (a<sub>4</sub>) the polymer jet shown moving downward because of the applied electrical field; (a<sub>5</sub>) the syringe needle, droplet and cone of continuous NFES; (a<sub>6</sub>) the as-spun fibers from (a<sub>5</sub>); (b) orderly patterned nanofibers; and (c) the dependence of nanofiber diameters on (c<sub>1</sub>) applied voltage, (c<sub>2</sub>) polymer concentration, and (c<sub>3</sub>) needle-to-collector distance. Reproduced with permission from ref 46. Copyright 2008 American Institute of Physics.

technique were further demonstrated via depositing diverse orderly patterns (like a three-character “Cal”, a grid pattern and a triangular pattern, as shown in Figure 3b) with the help of a programmable  $x$ - $y$  stage. Furthermore, systematic experiments have proved that the diameter of as-spun nanofibers can be controlled by adjusting various operating parameters, such as spinning voltage, polymer concentration and needle-to-collector distance (Figure 3c).

In 2014, a similar technique was reported to fabricate various PVDF micro/nano structures, such as straight and continuous lines, arc lines, parallel lines and beads-on-string structures.<sup>54</sup>

The key point of the modification was that an acupuncture needle tip was used to draw a polymer jet from the charged droplet to initiate electrospinning process. This mechanical way allows a lower electric field to direct write fiber structures. The comparison for the fabrication viability of direct-writing PVDF micro/nanostructures between conventional NFES and modified NFES was carried out as well. Besides, patterns on rigid or flexible substrate for various applications have been constructed by finely adjusting the key parameters of needle-to-collector distance, speed of movable collector, and solution property.

On the basis of the former experiment, line-type electrospun nanofibers can be controlled by managing the CMS to match with the electrospinning speed in NFES. Deposition behavior of coiled nanofibers electrospun by NFES has been demonstrated by both experiment and simulation.<sup>44</sup> Experimental results showed that with the decreasing of CMS, nanofibers shaped in straight line, wavy line, single-circle coil and multicircle coil could be fabricated in turn, which were in good agreement with the calculated behaviors in simulation (Figure 4). The reported paper concluded that the main influence for charged jet's whipping motion in NFES was the imbalanced charge repulsive force in landed nanofiber, in turn, the landed nanofiber with less charge could provide a guidance for the later nanofiber, this dual function ultimately led to the deposition of layer by layer and multicircle coil nanofibers. The reported experiment and simulation model represented a well control technology for the motion and deposition behavior of single nanofiber.

Although some demonstrations of NFES have been carried out to achieve a possibility of scalable precision alignment of polymeric nanofibers for a restricted or a large area deposition, it is still difficult to realize controlled continuous patterning of fibers on three-dimensional (3D) substrates due to the patterning perturbations and bending instabilities under the high electric field strength. To solve this problem, a method of continuously patterning polymeric nanofibers on 2D and 3D substrates (Figure 5) by low-voltage (lower than 600 V) NFES was reported by Bisht et al.<sup>47</sup> Furthermore, the fabricated nanofibers could be coated with metal to function as sensing elements and connectors on 3D microstructures. The key advance for lowering spinning voltage and increasing patterning control was the introduction of a superelastic polymer ink which contained long entangled polymer chains to bear enormous strains without breaking,<sup>55–57</sup> so the continuity of the electrospun polymer jet could be facilitated.<sup>58</sup>

**2.3. Melt NFES.** Just like TES, besides solution NFES, there also exists melt NFES. Melt NFES shares the same advantages with traditional melt electrospinning, which are solvent-free, high

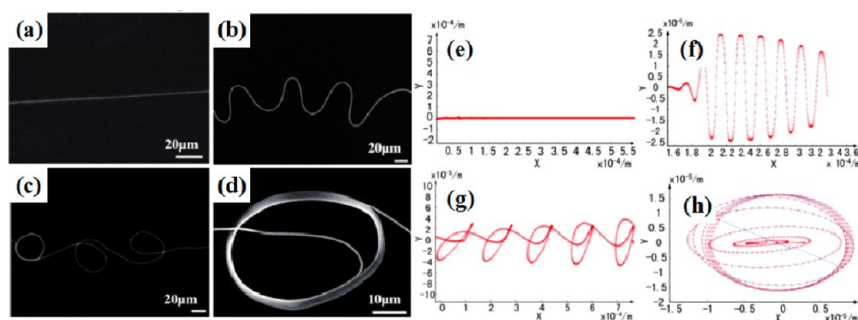


**Figure 4.** (a–d) NFES nanofibers shaped in straight line, wavy line, single-circle coil and multicircle coil under different CMS of 0.35, 0.25, 0.15, and 0.05 m/s, respectively; (e–h) simulation results from the computational model under different CMS of 0.4, 0.25, 0.1, and 0.05 m/s, respectively. Reproduced with permission from ref 44. Copyright 2010 IEEE.

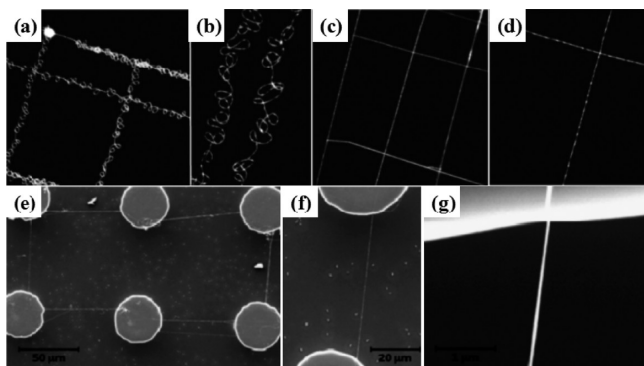


**Figure 5.** Deposition pattern of nanofibers on 2D and 3D substrates. (a, b) snakelike pattern of nanofibers prepared by low-voltage NFES of 2 wt % PEO at 600 V; (c, d) straight aligned pattern of nanofibers prepared by low-voltage NFES of 2 wt % PEO at 300 V; (e, f) suspended nanofibers of 2 wt % PEO on carbon micropost arrays at 300 V; (g) close up of the suspended nanofiber. Reproduced from ref 47. Copyright 2011 American Chemical Society.

yield and low environmental pollution. But for the short spinning distance, melt NFES also shares the same disadvantages with NFES. The fibers reach the collector before further stretching and thinning, which makes the diameters of collected fibers larger than traditional melt electrospinning. Relevant details of melt NFES, which is mainly applied to additive manufacturing of scaffolds, will be discussed in the next section about applications in tissue engineering.<sup>33,34,59–61</sup> As is known to counterparts that the techniques of higher resolution additive manufacturing are widely needed for tissue engineering, filters, fabrics, membranes and catalysts.<sup>62–65</sup> Compared with the common additive manufacturing approaches such as two-photon lithography, selective laser sintering, stereolithography and fused deposition modeling,<sup>66–69</sup> direct-writing melt NFES combined with automated laterally translating collection system allows the predictable deposition and fabrication of scaffolds with controllable architectures to be realized in a lower-cost and easier-operation way. Figure 6 shows some structured fibers fabricated by combining melt electrospinning with direct writing.

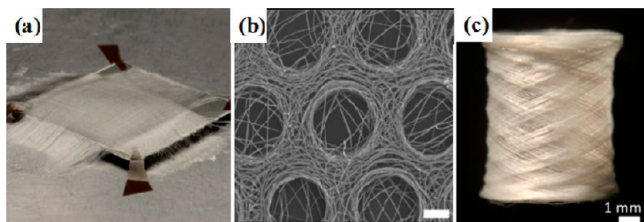


**Figure 6.** Some fiber structures fabricated via combining melt electrospinning with direct writing. (a) scaffold with 180 fiber layers. Reproduced with permission from ref 59. Copyright 2014 Elsevier B.V. (b) Patterned mesh fibers. Reproduced with permission from ref 60. Copyright 2014 Elsevier B.V. (c) Tubular scaffolds of PCL fibers. Reproduced with permission from ref 61. Copyright 2012 AIP.

**2.4. Electrospun Materials.** Many materials with different chemical and physical properties as well as the potential and practical applications have been used in NFES. For example, PEO is one kind of thermoplastic material, with a highly ordered structure, can be completely soluble in water, which has been applied in directly writing well-patterned fibers by NFES.<sup>28,38,46,47,52,53</sup> PVP can be soluble in water and a variety of organic solvents, with good moisture absorption, film formation,

complexation and physiological compatibility, which has been widely used in the initial stage to explore the spinning parameter.<sup>50</sup> PVP also have been reported as cosolvent together with other functional materials in NFES for the good chemical and physical properties.<sup>70,71</sup> Polycaprolactone (PCL) has good biodegradability, biocompatibility and nontoxicity, is widely used as biodegradable materials. Patterned PCL<sup>33,34,60,61</sup> and sugar-PCL core-shell fibers<sup>72</sup> prepared by NFES have been used in tissue engineering. Polystyrene (PS) is one kind of excellent insulation materials, which is colorless and transparent, chemically stable. Hierarchically buckled patterned PS fibers have been prepared by NFES.<sup>73</sup> Piezoelectric polyvinylidene fluoride (PVDF) is a kind of piezoelectric, high strength and corrosion resistant materials, which also has been widely used in NFES.<sup>29,74,75</sup> In addition to the above several common materials, poly(2-ethyl-2-oxazoline) (PEtOx) fibers,<sup>59</sup> and poly[2-methoxy-5-(2-ethylhexyloxy)-1,4-phenylenevinylene] (MEH-PPV),<sup>76</sup> fibers also have been used in NFES.

**2.5. Assembly of NFES Fibers.** NFES technique has got rapid development in recent years, it not only can be applicable to different materials, but also can fabricate various nanofiber structures to fit into multiple applications, such as individual fibers shaped in straight, waved or coiled line; parallel fibers shaped in straight or arc arrays; patterned fibers shaped in intersecting perpendicular or triangular arrays. After that, more and more structures have been successfully fabricated via NFES, as shown in Table 3.

Notably, in Table 3, the aligned and patterned core-shell structured fibers (Figure 7a) were fabricated via coaxial NFES.<sup>72</sup> Besides, except parallel and latticed patterns, hierarchically buckled fibers via NFES could be assembled in fiber balls consisting of stacked coils,<sup>73</sup> as shown in Figure 7b. In addition, besides the ordinary NFES approaches, a counter electrode/substrate technique was applied to realize low-voltage precision deposition,<sup>82</sup> and the nanofiber patterns were illustrated in Figure 7c.

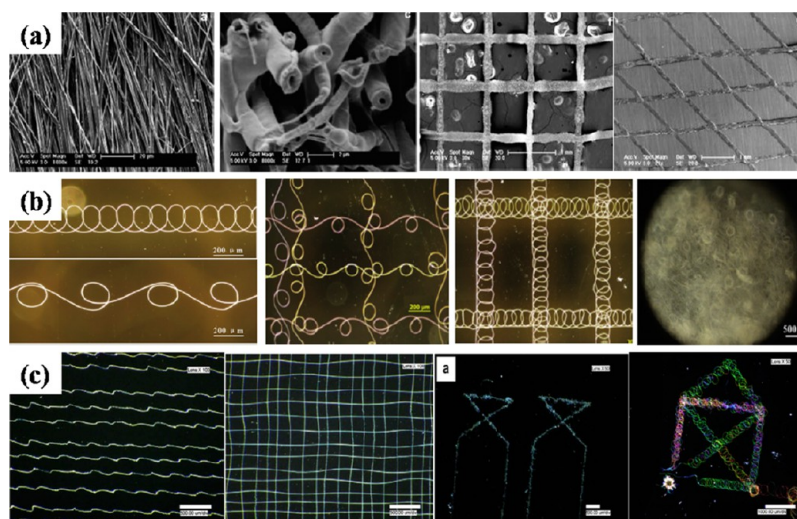
The interesting fibrous structures produced by NFES are mainly benefited from the smaller needle-to-collector distance and the 2D motion platform. The bending instability in spinning is significantly restricted by the smaller spinning distance, so the fibers could be deposited in straight-line stage with a controllable mode. Meanwhile, the 2D motion platform helps the fibers deposit in predesigned trajectory. Besides, the moving speed of platform is an important factor in controlling the diameters and morphologies of fibers. Particularly, it can be seen from Table 3 that though the diameters of fibers fabricated by melt NFES are usually larger than solution NFES, it is more suitable to fabricate special 3D fibrous structures and scaffolds. These special structures fabricated by NFES will surely be explored in more and more applications, and some typical reports will be introduced in section 3.

**2.6. Modification in Apparatus.** Occasionally, large droplets would heteronomously drop to the collector and coat the as-spun nanofibers for the action of gravity in the conventional vertical NFES configuration. In order to observe the nanofibers distinctly, a horizontal NFES configuration was adopted to avoid the covering droplet.<sup>50</sup> Not only uniform fibers but also beaded fibers were fabricated via the horizontal NFES approach (Figure 8). Particularly, besides the formation mechanism, processing variables including spinning distance, collecting position, concentration and humidity have also been explored by a series of experiments.

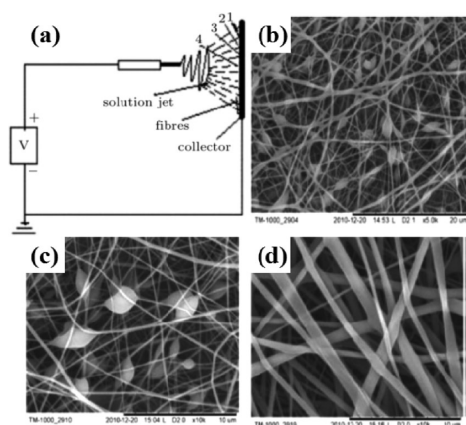


Table 3. List of Fiber Structures via Solution NFES and Melt NFES

| method        | fiber diameter             | structures   | polymer          | references                    |
|---------------|----------------------------|--|------------------|-------------------------------|
| solution NFES | 30 nm to 10 $\mu\text{m}$  | individual fiber shaped in straight, waved, or coiled line                 | PEO              | 28, 44, 77, 78                |
|               |                            | parallel fibers shaped in straight or arc arrays                           | PEO/PVDF/MEH-PPV | 30–32, 35, 36, 54, 76, 79, 80 |
|               |                            | patterned fibers shaped in intersecting perpendicular or triangular arrays | PEO/PVDF/MEH-PPV | 31, 46, 76                    |
|               |                            | fiber patterning on 3D substrate   | PEO              | 45, 47                        |
|               |                            | core-shell fibers  | sugar-PCL        | 72                            |
|               |                            | beads-on-string fiber structures   | PVP/PVDF         | 50, 54                        |
|               |                            | fiber patterning of hierarchical buckles                                   | PS               | 73                            |
|               |                            | 3D grid structure  | PVDF             | 81                            |
|               |                            | 3D grid structure  | PCL/PEtOx        | 33, 34, 59                    |
|               |                            | tubular scaffolds  | PCL              | 61                            |
| melt NFES     | 700 nm to 60 $\mu\text{m}$ | patterned mesh structure   | PCL              | 60                            |



**Figure 7.** (a) Aligned and patterned core-shell structured fibers via NFES. Reproduced with permission from ref 72. Copyright 2011 Elsevier Ltd. (b) Buckled patterns of PS fibers and fiber balls consisted of stacked coils. Reproduced with permission from ref 73. Copyright 2012 Elsevier Ltd. (c) Nanofiber patterns of low-voltage high precision deposition via a counter electrode/substrate technique. Reproduced with permission from ref 82. Copyright 2009 Elsevier Ltd.



**Figure 8.** (a) Schematic illustration of the horizontal setup for NFES; (b–d) SEM images of the uniform and beaded fibers. Reproduced with permission from ref 50. Copyright 2012 Chinese Physical Society and IOP Publishing Ltd.

The mentioned NFES approaches above are all assembled with single nozzle, however, due to the flow restriction, single-nozzle NFES system is unable to cope with mass production, which limits the industrial utilization in precision manufacturing.

To improve the high-precision production efficiency and rate, a multinozzle NFES system (Figure 9) was presented.<sup>83–85</sup> On the basis of the mutual influence of the charged jets under shifty

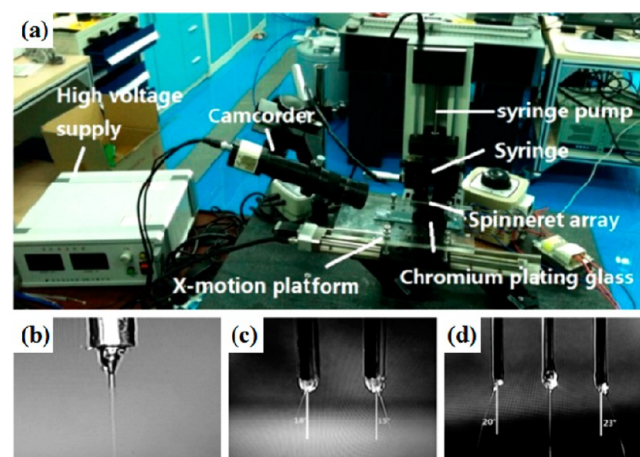


**Figure 9.** (a) Experimental device; (b–d) morphological illustration of liquid droplets for single-nozzle NFES, double-nozzle NFES, and triple-nozzle NFES, respectively. Reproduced with permission from ref 83. Copyright 2014 AIP.

conditions, the deposition characteristics of double-nozzle and triple-nozzle NFES systems have been demonstrated and analyzed. The mutual distance of deposition was mainly influenced by nozzle spacing and working distance, on the other hand, the influence of voltage was not particularly apparent, and analysis suggested that the main reason for these phenomena may be the function of Coulomb force. The experimental conclusions would provide a solid foundation for the manufacturing of multinozzle NFES.

Because of the unique features of structure and morphology, wavy fibers (mostly fabricated via electrohydrodynamic (EHD) jet printing, chemical vapor deposition and electrospinning) have great potency in many applications including stretchable electronic products, resonators, flexible displays, electronic skins and sensors.<sup>86–89</sup> In order to fabricate pattern-controllable wavy fibers, an approach of NFES combined with auxiliary electrodes (A–E) has been reported.<sup>77</sup> With the help of auxiliary electric field, fibrous morphology could be regulated easily, and the frequency of wavy fibers was matched with the frequency of alternating current power (ACP). This approach provided a significant convenience for fabricating zigzag fibers, which could be used to produce grating codes. Compared with the traditional preparation method of laser carve, which is very hard-operating and high-costing for gratings whose diameters are smaller than 5  $\mu\text{m}$ ,<sup>90</sup> this electric field assisted NFES (which is benefited from the precision controllability and the small diameter of fibers) is significantly capable for the construction of lines in the grating ruler. Besides, further investigation of the factors (including the nozzle-to-collector distance, nozzle-to-A–E distance, solution concentration, and charged jet morphology) that affected the deposition of wavy fibers and the experiment of electric field simulation were subsequently reported.<sup>78</sup> Except for the above modification in NFES, another secondary electric field NFES approach by using an auxiliary electrode ring was reported.<sup>91</sup> And the use of secondary electric field, which is perpendicular to fiber flight path, provides an effective way to improve the deposition resolution and control of fibers in NFES. Figure 10 shows the

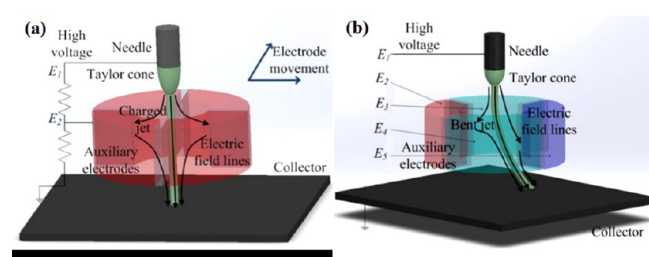


**Figure 10.** (a) Single potential piezo actuated electrode ring design and (b) multipotential stationary electrode ring design. Reproduced with permission from ref 91. Copyright 2015 ASME.

novel electrode designs of auxiliary electrode ring in NFES. In conclusion, the NFES apparatus are listed in Table 4.

### 3. APPLICATIONS

**3.1. Nanogenerator and Energy Harvester.** With increasing prominence of the energy problem, a considerable renewable energy source for various applications can be gained by capturing mechanical energy from surroundings. Besides large-scale power generators which convert energy from solar, waterfalls, wind, and ocean waves into electricity,<sup>92,93</sup> small-scale energy harvesters, which harvest energy by transforming mechanical vibration sources in building, automobiles, appliances, and human movements, have won tremendous attention.<sup>94,95</sup>

**Table 4.** A Summary of NFES Apparatus

| distinction | configuration                |                | first reported | reference |
|-------------|------------------------------|----------------|----------------|-----------|
| spinneret   | single-nozzle                | probe tip      | 2006           | 28        |
|             |                              | syringe needle | 2008           | 46        |
|             | multinozzle                  |                | 2015           | 83        |
| electrode   | auxiliary electrode pair     |                | 2015           | 77, 78    |
|             | auxiliary electrode ring     |                | 2015           | 91        |
| collector   | 2D moving platform           |                | 2006           | 28        |
|             | hollow cylindrical collector |                | 2014           | 75        |

For these mechanical energy harvesters, searching or designing applicable structural materials which can realize efficient conversion of mechanical energy into electricity is an essential matter.<sup>29</sup> Notably, energy explored in nature are highly time and location dependent. Thus, as the increasing popularity of independently self-sufficient portable smart electronics, self-powered nanosystems have attracted widespread attention, including piezoelectric nanogenerators (NGs) based on ZnO nanowire arrays<sup>96,97</sup> and electrospun piezoelectric PVDF nanofibers.<sup>98–101</sup>

One direct-write piezoelectric PVDF nanogenerator (NG) with high energy conversion efficiency has been reported.<sup>29</sup> In this work, NFES combining *in situ* mechanical stretch and electrical poling were utilized to direct write PVDF nanofibers to fabricate a NG. As shown in Figure 11, the PVDF nanofibers were directly written on a flexible plastic substrate, then, a piezoelectric potential generated as the substrate was bended by an axial stress. During the repeated stretching and releasing process, both the current and voltage could be recorded. Particularly, the electrical outputs of piezoelectric responses could be enhanced by increasing the numbers of the arranged nanofibers. High energy conversion efficiency and integratability with other micro/nanomanufacturing processes were featured in the reported NG which could be the basis for an integrated power source in portable electronics and wireless sensors. Besides, the same research team reported large array electrospun PVDF nanogenerators on a flexible substrate.<sup>80</sup>

Moreover, a direct-write, massively parallel aligned *in situ* poled PVDF microfibers-based harvester via NFES was illustrated in 2013.<sup>74</sup> On this basis, a direct-write and *in situ*

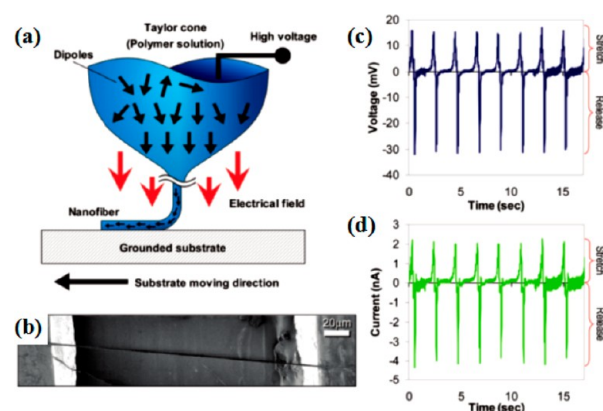


**Figure 11.** Piezoelectric PVDF nanogenerator. (a) NFES combining *in situ* mechanical stretch and electrical poling to create and place PVDF nanogenerators on a substrate; (b) SEM image of a nanogenerator consisted of a single PVDF nanofiber, two contact electrodes, and a plastic substrate; (c and d) output voltage and current under applied strain at 2 Hz. Reproduced with permission from ref 29. Copyright 2010 American Chemical Society.



poled PVDF NG was investigated for wearable and muscle-driven applications.<sup>30</sup> Extensive PVDF nanofiber arrays were fabricated on a flexible PVC substrate (equipped with different units of parallel electrode pairs) via NFES (Figure 12). In serial

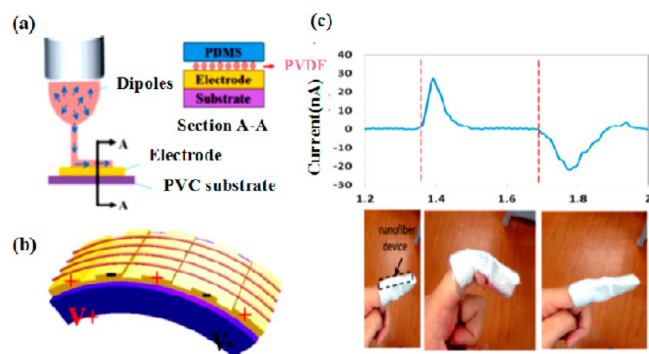


**Figure 12.** (a) Schematic illustration of the PVDF fibers-based NG, the fibers were deposited onto a flexible PVC substrate equipped with parallel electrode pairs to construct the NG; (b) mode of schematic deformation; (c) output current under the finger was bending-releasing at  $\sim 45^\circ$ . Reproduced from ref 30. Copyright 2015 American Chemical Society.

connections, as the number of stacked NGs increased to 3, the maximum output voltage and current could up to 20 V and 390 nA, respectively. When the nanofiber-based device was attached on the human finger, the output voltage and current could reach 0.8 V and 30 nA under bending-releasing at  $\sim 45^\circ$ . Furthermore, they also integrated a hybrid energy cell based on the nanofibers to harvest mechanical energy. For future wearable electronics, the fabricated nanofiber-based NGs and hybrid cell could provide a renewable energy source which could collect energy from human-based mechanical motion with extremely small amplitude.

Excepting the above NGs fabricated by NFES, due to the positive influence of NFES process on the piezoelectric and mechanical properties of PVDF/PMLG (poly( $\gamma$ -methyl L-glutamate)) composite fibers, a flexible PVDF/PMLG energy harvester which can capture ambient energy with a maximum peak voltage of 0.08 V has been reported.<sup>102</sup> The power of the harvester was 637.81 pW, and the energy conversion efficiency was 3.3%, compared with the corresponding pure PVDF and pure PMLG harvesters, this efficiency was three times higher. In 2013, Liu et al. demonstrated a modified hollow cylindrical near-field electrospinning (HCNFES) to fabricate PVDF energy harvesters characterized with excellent output properties.<sup>75</sup> Oriented fibers with high structure density were directly written on a rotating glass tube coated by copper foil via HCNFES. Then the piezoelectric PVDF fibers were packaged on a PFT substrate to design an energy harvester. The superiority of HCNFES is that the strong mechanical stretching generated from the rotating hollow cylinder and the high electrical field help the dipoles align along a uniform direction which enables the PVDF fibers have a good piezoelectric property. Meanwhile, the strong mechanical stretching in HCNFES could control the fibers characterized with smooth surface, smaller diameter and high structure density.

**3.2. Tissue Engineering.** From a biological perspective, almost all of the human organs and tissues like bone, muscle, blood vessel, cartilage, skin and collagen are existed in nanofibrous structures or forms.<sup>5</sup> For the malfunctioning tissues or organs in human body, one of the fundamental challenges in

treatment is to design and manufacture ideal scaffolds for cell's proliferation, differentiation and migration. Herein, a controllable and reliable preparation process is one of the key elements in furthering tissue engineering and regenerative medicine research. Examples include: phase separation, freeze-drying, particulate leaching, solvent casting and electrospinning.<sup>103–109</sup> However, almost all these processes have their own limitations mainly regarding the capacity of precisely control scaffold's geometrical morphology, pore size and interconnectivity,<sup>62,105</sup> which should well match the structure and biological functions of the natural extracellular matrix.<sup>5</sup> Researches show that human cells can attach and organize appropriately around fibers with diameters smaller than the corresponding cells.<sup>110</sup> For these reasons, electrospun fibrous scaffolds with suitable porosity, nanoscale topography and interconnectivity provide an ideal template for tissue engineering. The above common properties of electrospun fibers combines the superiority of precisely controllable deposition make NFES exerts a widespread potential application in biomedical engineering.<sup>31–34</sup>

NFES was utilized by Fuh et al. to fabricate highly aligned chitosan nanofibers (CNF) with prescribed positioning density in direct-write patterns.<sup>31</sup> In their experiments, the parallel-aligned CNF greatly influenced cell spreading, and the morphology of human embryonic kidney (HEK) cells were successfully reconstructed on these patterned CNF. Because the obtained direct-write patterns are markless, low-cost and can be fabricated easily, this research provides a promising method to study cell-based research in bioengineering. Then on this basis, Fuh et al. have directly written biodegradable alginate fibers via NFES to control the cell orientation.<sup>32</sup> To control the deposition sites of NFES fibers, a conductive substrate is necessary, so they used a homemade conductive polypyrrole (PPy) film as substrate. The other reason to use PPy film is that PPy is an appropriate substrate to sustain cell growth, while alginate is an unfavorable material for cell adhesion,<sup>111</sup> these two materials provide a high contrast pattern for the guidance of cell extension. Compared to traditional electrospun fibers which were randomly deposited, NFES fibers primely guided the extension of HEK 293T cells, and the cell alignment increased with the decrease of fibers interspace (Figure 13a). Besides, in the research, combining the alternation of ion-cross-linking, the alginate fiber patterns could degrade gradually with time, so more space for cell growth was provided after the guidance for cell extension in the initial stage (Figure 13b).

For the application of bioengineering, besides solution NFES, there also exist melt NFES. One direct-writing melt electrospinning, which can prepare 3D complex porous structures of poly( $\epsilon$ -caprolactone) (PCL) fibers for biomedical applications that allow cell and tissue invasiveness, has been reported in 2011.<sup>33</sup> As for this approach, the voltage and collector distance were fixed at 12 kV and 30 mm, which were dramatically lower than traditional melt electrospinning. In addition, consistently laying melt electrospun fibers on top of each other to fabricate 3D periodic lattices (Figure 14) had been demonstrated for the first time in the paper. To some extent, this direct writing melt electrospinning can help to bridge the gap between solution electrospinning and direct-write additive manufacturing processes.

For *in vitro* research, another layer-by-layer submicron PCL filaments structure was directly written to prepare discrete 3D scaffolds (Figure 15a) via melt electrospinning (optimal parameters: accelerating voltage 2.9 kV, collector distance 1.5 mm, heating temperature 109  $^\circ\text{C}$ ).<sup>34</sup> The ultrafine filaments with



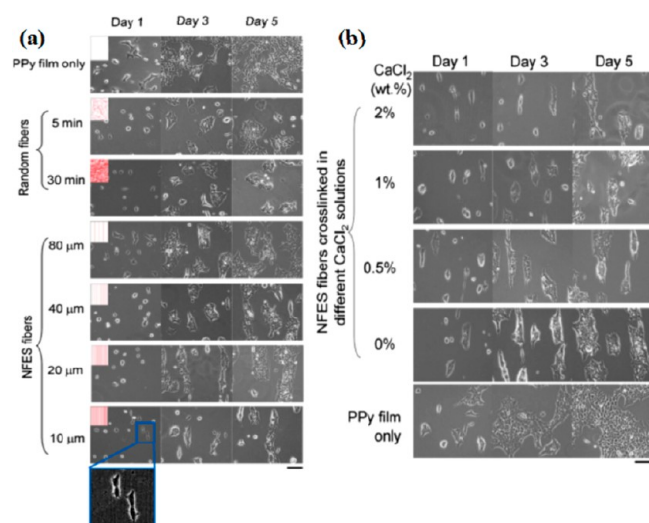


**Figure 13.** (a) Distribution and morphology of HEK 293T surface cells seeding on PPy films for randomly deposited alginate fibers and NFES alginate fibers; (b) cell alignment on NFES alginate fibers partially cross-linked in different concentrations of CaCl<sub>2</sub>. Reproduced with permission from ref 32. Copyright 2016 Elsevier B.V.

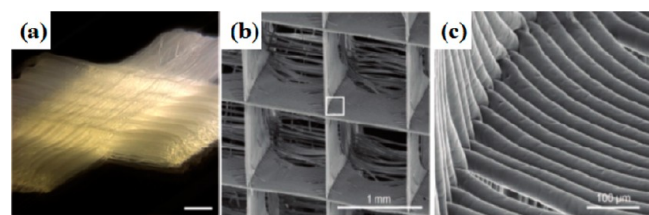


**Figure 14.** (a) Photograph of 3D porous structures of PCL fibers; (b and c) SEM images of the stacking and interweaving of fibers. Reproduced with permission from ref 33. Copyright 2011 WILEY-VCH Verlag GmbH & Co. KGaA, Weinheim, Germany.

smallest diameter of  $817 \pm 165$  nm were deposited on a NCO-sP(EO-*stat*-PO)-coated glass slide to form box-structures for cell adhesion tests. Paradigmatic experiment showed that hMSCs (human mesenchymal stromal cells) tended to keep away from the NCO-sP(EO-*stat*-PO) coated surface to adhere and grow along the filaments (Figure 15c–f). And interestingly, when illuminating the glass slide, there appears an optical effect on box structured scaffolds due to their high deposition accuracy (Figure 15b).

**3.3. Wearable Devices.** Because of the special sensitivity, portability, durability, and mechanical property, flexible wearable devices could work in various working environments, and have great potential to promote the fusion of human and information.<sup>112</sup> The increasing popularity of these advantages makes flexible wearable devices a hot destination for device manufacture, such as electronic skin,<sup>113</sup> flexible screens,<sup>114</sup> robot joints,<sup>115</sup> and warning of natural disaster.<sup>116</sup>

Well-aligned composite PVDF/MWCNTs (multiwalled carbon nanotubes) fibers with high density, smooth surface, and high nucleation (oriented  $\beta$ -crystalline phase along the fiber axis) were directly electrospun through HCNFES (Figure 16a).<sup>35</sup> Because of the combine of high uniaxial stretching and electrical poling in HCNFES process, the composite fibers are characterized with smaller diameter and good piezoelectricity. Subsequent research showed that the mechanical properties of the fibers could be improved by adding a small amount of

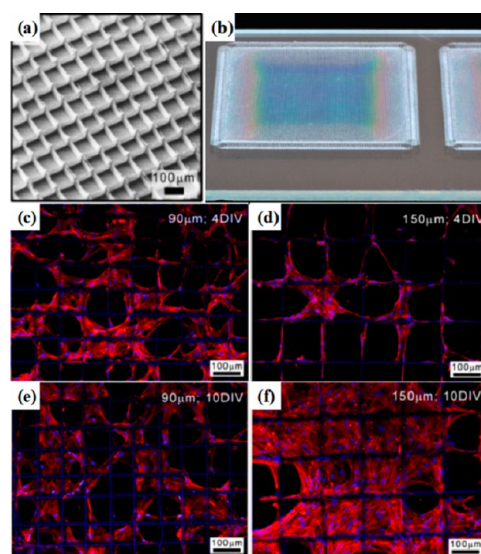


**Figure 15.** (a) SEM image of box-structure of PCL ultrafine filaments; (b) optical effects on box structured scaffolds; (c–f) *in vitro* experiments on scaffolds for cell adhesion tests, hoechst staining for nuclei also rendered the fibers blue. Reproduced with permission from ref 34. Copyright 2015 IOP Publishing Ltd.

MWCNTs. To explore their feasible applications, the orderly fibers were packaged on a thin flexible polymer substrate to assemble a wearable sensing device. Through testing the output property, the device showed a high piezoelectricity and durability (Figure 16b), which were applicable for highly durable wearable sensors. With outstanding piezoelectricity and mechanical property, the HCNFES PVDF/MWCNTs fibers could be useful in electromechanical actuators, energy transducers and functional nanowire clothes.

A flexible strain sensor based on electroconductive polymer nanofibers, which can be used for flexible and wearable devices has been demonstrated by Shen et al.<sup>36</sup> As a preliminary, the researchers synthesized soluble PPy and direct wrote multiple and aligned PPy/PEO nanofibers on a flexible substrate by NFES process. The substrate was preprocessed with a 5-μm-wide gap to separate two gold pads. By controlling and placing the spinning tip in 3D space, arbitrary contours on wearable devices via this process. According to the output electrical signals, the wearable sensor was specifically sensitive to stress applied along the fiber direction.

**3.4. Conductive Electrodes.** By means of NFES, a preparation method of using silver nanoparticles (AgNPs) and silver nanowires (AgNWs) to fabricate conductive fibers and films has been reported.<sup>70</sup> The fibers and films with superior conductivity and transmissivity could be used as transparent conductive electrodes. Details of the process and mechanism were investigated in another paper.<sup>71</sup> In the papers, AgNPs and AgNWs were synthesized via polyol reduction process, then, the PVP/AgNWs fibers were electrospun by NFES. Through the centrifugation and spin coating process, pure AgNWs transparent films were obtained finally. When the thickness of the film was 1.6 μm, the corresponding sheet resistance was 0.032 Ω/sq, which was superior to the commercial ITO. And analysis found that there was 5% decrease in transmissivity for every 100 Å increase in thickness. This reported process and result provided a potential application in transparent conductive electrodes. Besides, conducting microscale electrodes of transparent silver hybrid films was successfully fabricated on insulating substrate via NFES.<sup>117</sup>

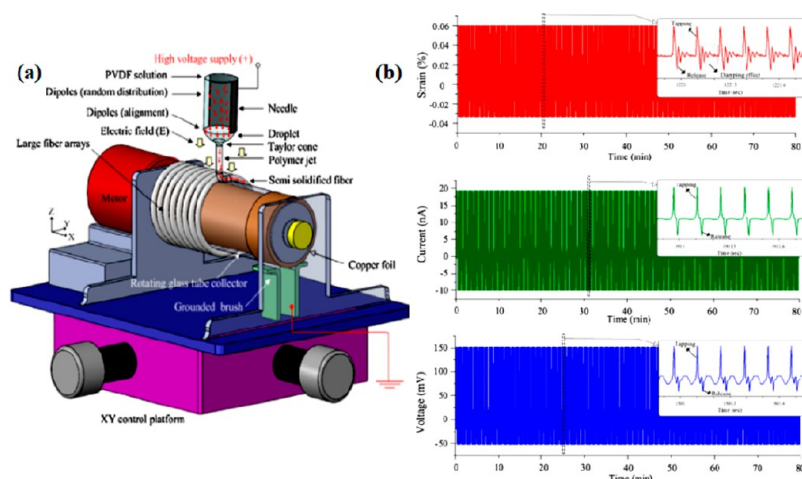


**Figure 16.** (a) Schematic illustration of the HCNFES process; (b) the measured strains, output voltages and currents of the wearable sensor under continuous tapping-release for 80 min. Reproduced with permission from ref 35. Copyright 2015 Elsevier B.V.

Usually, looking for effective electrodes is one of the key factors to realize high performance for electromechanical systems. High aspect-ratio 3D conductive grid electrodes for supercapacitor (Figure 17) have been fabricated by NFES.<sup>81</sup> The direct-write 3D structures were electrospun on papers, where the structures could be mechanically separated for various applications. After that, the detached structures were dipped into CNTs (carbon nanotubes) ink and followed by a drying treatment. After the dip-and-dry process, the 3D structure's original shape was maintained, and the conductivity could achieve ca.  $850 \text{ S m}^{-1}$ . Thus, the flexible CNTs coated PVDF grid-structured conductive electrodes were assembled to be a micro-supercapacitor. The capacitance of the supercapacitor with 3D grid-structure electrodes was about 25 times larger than a control cell.

**3.5. Nanochannel.** As one of the fundamental building blocks for micro/nanofluidic, electronic devices and circuits, nanogap electrodes have drawn great interests for their superior properties and application prospect.<sup>118</sup> Li et al. have successfully fabricated nanochannels via NFES, which were available to prepare electrode gaps and fluidic channels with low cost, water scalability, and well-defined features.<sup>39</sup> In the reported process,

nanofibers were directly fabricated on a substrate by NFES to be used as sacrificial templates, then, a coating process and a removal of sacrificial nanofibers were followed to obtain orderly and patterned nanochannels (Figure 18). This method that

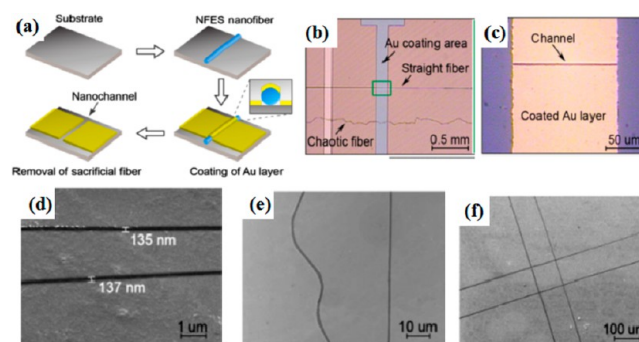


**Figure 18.** Nanochannels: (a) schematic diagram of nanochannel fabrication process; (b and c) optical images of NFES fibers and the fabricated channel; (d–f) parallel, wavy, and grid channel, respectively. Reproduced with permission from ref 39. Copyright 2012 Springer-Verlag.

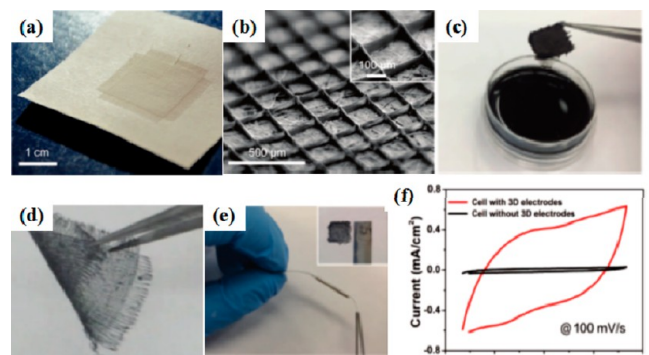


**Figure 17.** (a) Optical image of a 3D grid structure on paper substrate; (b) SEM image of a 3D grid structure for 20 layers of PVDF fibers; (c) the dip-coating process in the CNTs ink solution; (d) a 3D grid structure after coating with CNTs; (e) assembled microsupercapacitor with 3D grid-structure electrodes; (f) C–V results of micro-supercapacitors with and without 3D grid-structure electrodes. Reproduced with permission from ref 81. Copyright 2016 IEEE.

combined NFES and conventional MEMS fabrication techniques opened a new-type and low-cost approach in micro/nano manufacturing. In addition, Lee et al. once employed a similar method to fabricate chip-to-chip fluidic connectors via NFES. By integration with the subsequent coating process and sacrificial layer etching process, micro/nanofluidic channels with inner diameter of  $50 \text{ nm} \sim 5 \text{ } \mu\text{m}$  were formed between chips.<sup>40</sup> This preparation approach could enable on-chip and off-chip fluidic transportations apply in MEMS field (including BioMEMS and microfluidics applications).

**3.6. Photodetector.** High-performance photodetector is one of the most crucial parts in high-speed optical communication and environmental sensing. Liu et al. demonstrated an all-printable band-edge modulated ZnO nanowire photodetector on flexible substrates.<sup>119</sup> The fabrication system was retrofitted from an inkjet printer to combine inkjet printing and high throughput electrospinning where the collector distance was  $\sim 30 \text{ } \mu\text{m}$ . Systematic study showed that their ZnO nanowire photodetector was qualified with ultrahigh photoconductive gain, detectivity and responsivity at low bias (Figure 19). The



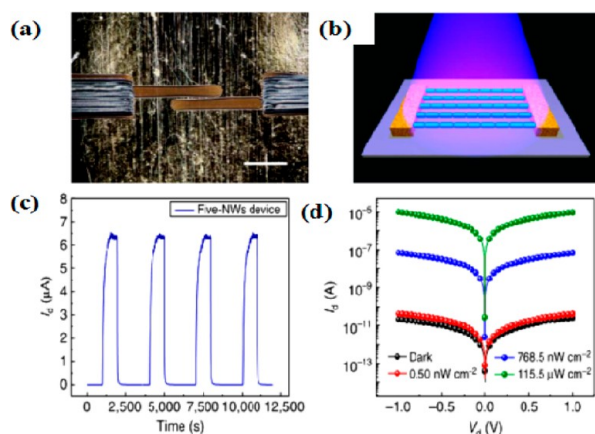


**Figure 19.** ZnO nanowire photodetector: (a) optical image of the photodetector with scale bar of 50  $\mu\text{m}$ ; (b) schematic diagram of a photodetector under UV illumination; (c) and (d) time domain photoresponse and  $I$ – $V$  curves of a photodetector at +1 V bias voltage. Reproduced with permission from ref 119. Copyright 2014 Macmillan Publishers Limited.

developed fabrication method will provide a guideline to design high-performance flexible and portable optoelectronic devices in the future.

**3.7. Field-Effect Transistor.** A single ZnO nanofiber-based field-effect transistor had been reported in 2013.<sup>37</sup> The preparing technique they adopted was electrohydrodynamic direct-writing (EDW), which was similar to or belongs to NFES in a sense. In the process, the applied voltage was 2 kV, and the nozzle-to-substrate distance was 2 mm. The ZnO nanofibers fabricated by EDW were not merely deposited individually but could be assembled into complex patterns for relevant device architectures. For demonstrating, a single ZnO nanofiber was patterned on a pair of Au electrodes, which were equipped on a preprocessed silicon substrate, to prepare a field-effect transistor (FET) by

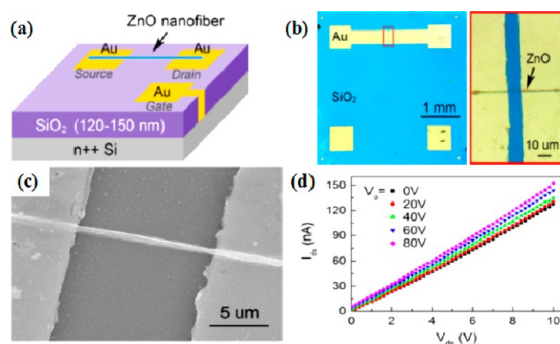


**Figure 20.** (a) Schematic of the FET made of single direct-written ZnO nanofiber; (b) photograph of the FET device; (c) SEM image of the ZnO nanofiber crossing two Au electrodes; (d) gate-dependent  $I$ – $V$  characteristics of the single ZnO nanofiber FET. Reproduced with permission from ref 37. Copyright 2013 Elsevier B.V.

EDW and calcining processes (Figure 20).  $I_{\text{ds}}$  of the FET could be enhanced by applying positive  $V_g$ , and the output characteristic was satisfied with the  $n$ -channel FET behavior. Significantly, the simple, low cost, robust controllable deposition and the visible real-time monitoring provide an effective approach to integrate functional nanofibers into nano/microelectronic devices.

**3.8. Conductor–Insulator–Conductor Multilayer Interconnection.** Later, the same research team printed a conductor–insulator–conductor multilayer interconnection via electrohydrodynamic (EHD) printing (similar to EDW).<sup>38</sup> They printed silver (the applied voltage was 1.2 kV) as the bottom and top conductor track and polyvinylpyrrolidone (PVP) (the

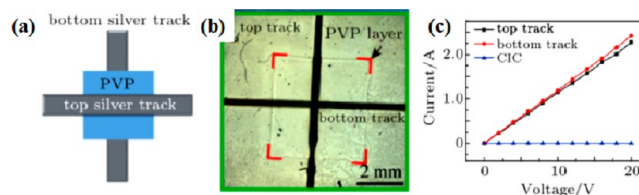


**Figure 21.** Conductor–insulator–conductor multilayer interconnections: (a) schematic of the multilayer interconnection; (b) a printed multilayer interconnection; (c) electric properties of the multilayer interconnection. Reproduced with permission from ref 38. Copyright 2014 Chinese Physical Society and IOP Publishing Ltd.

applied voltage was 2.5 kV) as the sandwiched insulator layer (Figure 21). To increase conductivity, the multilayer interconnection was sintered at 150  $^{\circ}\text{C}$  for 10 min. The average resistivity values of the bottom silver track and the top silver track were  $1.34 \times 10^{-7} \Omega\cdot\text{m}$  and  $1.39 \times 10^{-7} \Omega\cdot\text{m}$  respectively, and electric current could not pass from one conductor layer to the other one. For printed electronic devices, this EHD printing technique provides an alternative, fast, and cost-effective way to prepare conductor–insulator–conductor multilayer interconnections.

**3.9. Light-Emitting Nanofibers.** Although NFES has been demonstrated to synthesize and deposit various nanofibers with high precision, applying NFES to light-emitting conjugated polymers remains unexplored. Light-emitting conjugated polymers have great values in optoelectronic applications, and many of them have reached commercialization.<sup>120–122</sup> However, due to the low molar mass, chain rigidity and limited solubility, conjugated polymers cannot be easily electrospun, and it is difficult to integrate individual light-emitting nanofibers with optoelectronic devices by TES system.<sup>123–126</sup> From these reasons, Camillo et al. fabricated well-aligned light-emitting conjugated polymer of poly[2-methoxy-5-(2-ethyl-hexyloxy)-1,4-phenylenevinylene] (MEH-PPV) nanofibers with diameters down to 100 nm by NFES.<sup>76</sup> Compared with reference films, the electrospun fibers exhibit blue-shifted photoluminescence (PL) (with emission peak of 560 nm) and self-waveguiding of the emission (Figure 22). In perspective, these results open an interesting approach for the fabrication of arrayed architectures and photonic circuits composed of light-emitting nanofibers; precisely positioning and integrating conjugated polymer nanofibers into light-emitting devices could be promoted as well.

## 4. SUMMARY AND OUTLOOK

In this review, the recent research advances of NFES were briefly summarized. Besides, other aspects regarding the mechanism, advantages and some primary limitations, as well as the development tendency have also been discussed. The encouraging achievements highlighted in this article have shown practicality and promising development potential for NFES (with characteristics of controllable deposition, low cost, and easy operation) in the preparation and integration of arranged fibers.



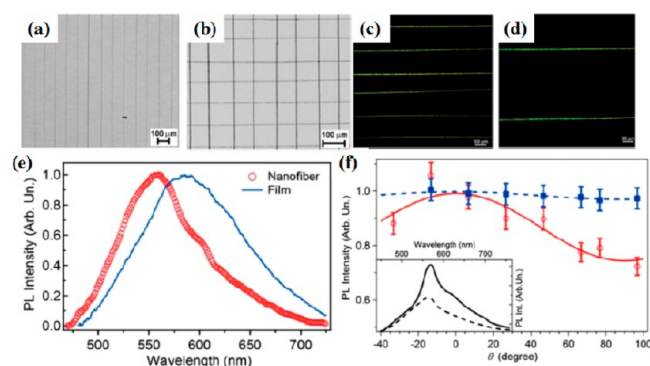


**Figure 22.** (a, b) Optical images and (c, d) confocal fluorescence images of arrayed MEH-PPV nanofibers by NFES; (e)  $\mu$ -PL spectra of a single nanofiber (open circles) and a reference film (continuous line); (f) PL intensity (empty circles) vs the incident laser polarization angle,  $\theta$ , measured with respect to the fiber longitudinal axis. Reproduced with permission from ref 76. Copyright 2013 The Royal Society of Chemistry.

As a simple and efficient technique to fabricate position-controlled fibers, NFES has become a growing focus in views of material scientists and biologists. With the development of NFES, both the precursive materials and the electrospun nanofibers are specialized toward diversification, functionalization and practicalization. Significantly, increasing the high-precision production rate of components, NFES opens an interesting perspective for the realization of controllable deposition and feasible integration of individual or arranged fibers with flexible and functional devices, which greatly expands its applications in energy harvesting, tissue engineering, wearable sensors, microelectronics, and MEMS structures.<sup>29–40</sup>

Gradually, NFES has got some new research progresses in different fields.<sup>127,128</sup> In the future, NFES will surely prove to be a promising fiber manufacturing candidate for a wide range of multiple and functional applications in nanostructures and devices, because NFES provides novel functionality through the powerful integration of nanofibers with nanodevices. In spite of the considerable advantages, NFES remains to be further improved. Future advances are potentially carried out from the following aspects: (1) deep researches on NFES mechanism including theoretical simulation and path planning technology to compensate the resulting error; (2) comprehensive combination of NFES with EDW technique or 3D printing to fabricate complex structures of functional devices;<sup>89</sup> (3) expanding developments for melt NFES to boost biological compatibility of structured nanofibers; (4) further exploration of potential applications; (5) commercialized NFES apparatus with features of miniaturization, integration, or high production.

## AUTHOR INFORMATION

### Corresponding Author

\*(Y.Z.L.) Fax: +86 532 85955977. Telephone: +86 139 5329 0681. E-mail: [yunze.long@163.com](mailto:yunze.long@163.com) or [yunze.long@qdu.edu.cn](mailto:yunze.long@qdu.edu.cn).

### ORCID

Yun-Ze Long: 0000-0002-4278-4515

### Author Contributions

<sup>†</sup>These two authors contributed equally to this work.

### Notes

The authors declare no competing financial interest.

## Biographies



Xiao-Xiao He received her BS degree from Qingdao University in 2015. Now she is studying for a master's degree at Qingdao University (with Prof. Yun-Ze Long). Her current scientific interests are focused on electrospinning, conductive nanocomposites, and their applications in flexible devices.



Jie Zheng received her MS degree from Qingdao University in 2013 and her PhD degree from Qingdao Institute of Bioenergy and Bioprocess Technology, Chinese Academy of Sciences, in 2016. Then she joined Qingdao University as a lecturer. Her current scientific interests are focused on nonwoven fibers and electrospinning.



Gui-Feng Yu received her MS degree from Sichuan University in 2005 and her PhD degree from Qingdao University in 2016 (with Prof. Yun-Ze Long). Her current scientific interests are focused on electrospinning, functional nanomaterials and their applications in nano-devices.



Xin Ning is a graduate of the Peking University with BS and MS degrees in Chemistry. He earned his PhD degree in Polymer Science and Engineering from Case Western Reserve University in the USA. He is currently a full Professor at the Qingdao University. He is also the director of the Industrial Research Institute of Nonwovens and Technical Textiles. Professor Ning's current research areas are nonwoven equipment, materials, and their applications.



Yun-Ze Long received his BS degree from the University of Science & Technology of China and PhD degree from the Institute of Physics, Chinese Academy of Sciences. Then he worked in Institut Matériaux Jean Rouxel, CNRS, France, as a postdoctoral Fellow. He has been with Qingdao University since December 2006, where he is currently a full Professor. From 2009 to 2011, he worked as a visiting researcher at the University of Sydney and Hong Kong University of Science & Technology. He has published more than 160 papers, and holds more than 50 Chinese patents. His research interests are focused on electrospinning, functional nanomaterials, and their applications.

## ■ ACKNOWLEDGMENTS

This work was supported by the National Natural Science Foundation of China (51373082 and 51673103) and the Taishan Scholars Program of Shandong Province, China (ts20120528).

## ■ ABBREVIATIONS

|       |                           |
|-------|---------------------------|
| 1D    | one-dimensional           |
| 2D    | two-dimensional           |
| 3D    | three-dimensional         |
| SES   | solution electrospinning  |
| MES   | melt electrospinning      |
| ACP   | alternating current power |
| AFM   | atomic force microscope   |
| AgNPs | silver nanoparticles      |

|         |   |
|---------|---|
| AgNWs   | silver nanowires  |
| CNF     | chitosan nanofiber  |
| CNTs    | carbon nanotubes  |
| CMS     | collector moving speed                                    |
| EDW     | electrohydrodynamic direct-writing                        |
| EHD     | electrohydrodynamic                                       |
| FET     | field-effect transistor                                   |
| HCNFES  | hollow cylindrical near-field electrospinning             |
| HEK     | human embryonic kidney                                    |
| hMSC    | human mesenchymal stromal cell                            |
| MEH-PPV | poly[2-methoxy-5-(2-ethylhexyloxy)-1,4-phenylenevinylene] |
| MEMS    | microelectromechanical system                             |
| MES     | melt electrospinning                                      |
| MWCNTs  | multiwalled carbon nanotubes                              |
| TES     | traditional electrospinning                               |
| NFES    | near-field electrospinning                                |
| NG      | nanogenerator   |
| PCL     | poly( $\epsilon$ -caprolactone)                           |
| PEO     | poly(ethylene oxide)                                      |
| PEtOx   | poly(2-ethyl-2-oxazoline)                                 |
| PL      | photoluminescence   |
| PMLG    | poly( $\gamma$ -methyl L-glutamate)                       |
| PPy     | polypyrrole   |
| PS      | polystyrene   |
| PVC     | polyvinyl chloride  |
| PVDF    | polyvinylidene fluoride                                   |
| PVP     | polyvinylpyrrolidone                                      |
| SEM     | scanning electron microscope                              |

## ■ REFERENCES

- (1) Huang, C. B.; Chen, S. L.; Lai, C. L.; Reneker, D. H.; Qiu, H.; Ye, Y.; Hou, H. Q. Electrospun polymer nanofibers with small diameters. *Nanotechnology* **2006**, *17*, 1558–1563.
- (2) Deitzel, J. M.; Kleinmeyer, J.; Harris, D.; Beck Tan, N. C. The effect of processing variables on the morphology of electrospun nanofibers and textiles. *Polymer* **2001**, *42*, 261–272.
- (3) Yu, G. F.; Yan, X.; Yu, M.; Jia, M. Y.; Pan, W.; He, X. X.; Han, W. P.; Zhang, Z. M.; Yu, L. M.; Long, Y. Z. Patterned, highly stretchable and conductive nanofibrous PANI/PVDF strain sensors based on electrospinning and *in situ* polymerization. *Nanoscale* **2016**, *8*, 2944–2950.
- (4) Yan, C. Y.; Wang, J. X.; Kang, W. B.; Cui, M. Q.; Wang, X.; Foo, C. Y.; Chee, K. J.; Lee, P. S. Highly stretchable piezoresistive graphene–nanocellulose nanopaper for strain sensors. *Adv. Mater.* **2014**, *26*, 2022–2027.
- (5) Huang, Z. M.; Zhang, Y. Z.; Kotaki, M.; Ramakrishna, S. A review on polymer nanofibers by electrospinning and their applications in nanocomposites. *Compos. Sci. Technol.* **2003**, *63*, 2223–2253.
- (6) Lang, C. H.; Fang, J.; Shao, H.; Ding, X.; Lin, T. High-sensitivity acoustic sensors from nanofibre webs. *Nat. Commun.* **2016**, *7*, 11108.
- (7) Sun, B.; Long, Y. Z.; Chen, Z. J.; Liu, S. L.; Zhang, H. D.; Zhang, J. C.; Han, W. P. Recent advances in flexible and stretchable electronic devices via electrospinning. *J. Mater. Chem. C* **2014**, *2*, 1209–1219.
- (8) Wang, Z. L.; Guo, R.; Li, G. R.; Lu, H. L.; Liu, Z. Q.; Xiao, F. M.; Zhang, M.; Tong, Y. X. Polyaniline nanotube arrays as high-performance flexible electrodes for electrochemical energy storage devices. *J. Mater. Chem.* **2012**, *22*, 2401.
- (9) Bhardwaj, N.; Kundu, S. C. Electrospinning: a fascinating fiber fabrication technique. *Biotechnol. Adv.* **2010**, *28*, 325–347.
- (10) Long, Y. Z.; Yu, M.; Sun, B.; Gu, C. Z.; Fan, Z. Y. Recent advances in large-scale assembly of semiconducting inorganic nanowires and nanofibers for electronics, sensors and photovoltaics. *Chem. Soc. Rev.* **2012**, *41*, 4560–4580.
- (11) Zhang, H. D.; Tang, C. C.; Long, Y. Z.; Zhang, J. C.; Huang, R.; Li, J. J.; Gu, C. Z. High-sensitivity gas sensors based on arranged

polyaniline/PMMA composite fibers. *Sens. Actuators, A* **2014**, *219*, 123–127.

(12) Kim, J. K.; Manuel, J.; Lee, M. H.; Scheers, J.; Lim, D. H.; Johansson, P.; Ahn, J. H.; Matic, A.; Jacobsson, P. Towards flexible secondary lithium batteries: polypyrrole-LiFePO<sub>4</sub> thin electrodes with polymer electrolytes. *J. Mater. Chem.* **2012**, *22*, 15045.

(13) Liu, S.; Liu, S. L.; Long, Y. Z.; Liu, L. Z.; Zhang, H. D.; Zhang, J. C.; Han, W. P.; Liu, Y. C. Fabrication of p-type ZnO nanofibers by electrospinning for field-effect and rectifying devices. *Appl. Phys. Lett.* **2014**, *104*, 042105.

(14) Teo, W. E.; Inai, R.; Ramakrishna, S. Technological advances in electrospinning of nanofibers. *Sci. Technol. Adv. Mater.* **2011**, *12*, 013002.

(15) Lyons, J.; Li, C.; Ko, F. Melt-electrospinning part I: processing parameters and geometric properties. *Polymer* **2004**, *45*, 7597–7603.

(16) Zhang, L. H.; Duan, X. P.; Yan, X.; Yu, M.; Ning, X.; Zhao, Y.; Long, Y. Z. Recent advances in melt electrospinning. *RSC Adv.* **2016**, *6*, 53400–53414.

(17) Brown, T. D.; Dalton, P. D.; Hutmacher, D. W. Melt electrospinning today: An opportune time for an emerging polymer process. *Prog. Polym. Sci.* **2016**, *56*, 116–166.

(18) Hutmacher, D. W.; Dalton, P. D. Melt electrospinning. *Chem. - Asian J.* **2011**, *6*, 44–56.

(19) Nagy, Z. K.; Balogh, A.; Dravavolgyi, G.; Ferguson, J.; Pataki, H.; Vajna, B.; Marosi, G. Solvent-free melt electrospinning for preparation of fast dissolving drug delivery system and comparison with solvent-based electrospun and melt extruded systems. *J. Pharm. Sci.* **2013**, *102*, 508–517.

(20) Liu, S. L.; Long, Y. Z.; Huang, Y. Y.; Zhang, H. D.; He, H. W.; Sun, B.; Sui, Y. Q.; Xia, L. H. Solventless electrospinning of ultrathin polycyanoacrylate fibers. *Polym. Chem.* **2013**, *4*, 5696–5700.

(21) He, H. W.; Wang, L.; Yan, X.; Zhang, L. H.; Yu, M.; Yu, G. F.; Dong, R. H.; Xia, L. H.; Ramakrishna, S.; Long, Y. Z. Solvent-free electrospinning of UV curable polymer microfibers. *RSC Adv.* **2016**, *6*, 29423–29427.

(22) Theron, S. A.; Yarin, A. L.; Zussman, E.; Kroll, E. Multiple jets in electrospinning: experiment and modeling. *Polymer* **2005**, *46*, 2889–2899.

(23) Li, D.; Wang, Y. L.; Xia, Y. N. Electrospinning of polymeric and ceramic nanofibers as uniaxially aligned arrays. *Nano Lett.* **2003**, *3*, 1167–1171.

(24) Li, D.; Wang, Y. L.; Xia, Y. N. Electrospinning nanofibers as uniaxially aligned arrays and layer-by-layer stacked films. *Adv. Mater.* **2004**, *16*, 361–366.

(25) Zhang, D. M.; Chang, J. Patterning of electrospun fibers using electroconductive templates. *Adv. Mater.* **2007**, *19*, 3664–3667.

(26) Yang, D.; Lu, B.; Zhao, Y.; Jiang, X. Fabrication of aligned fibrous arrays by magnetic electrospinning. *Adv. Mater.* **2007**, *19*, 3702–3706.

(27) Tokarev, A.; Trotsenko, O.; Griffiths, I. M.; Stone, H. A.; Minko, S. Magnetospinning of nano- and microfibers. *Adv. Mater.* **2015**, *27*, 3560–3565.

(28) Sun, D.; Chang, C.; Li, S.; Lin, L. Near-field electrospinning. *Nano Lett.* **2006**, *6*, 839–842.

(29) Chang, C. E.; Tran, V. H.; Wang, J. B.; Fuh, Y. K.; Lin, L. W. Direct-write piezoelectric polymeric nanogenerator with high energy conversion efficiency. *Nano Lett.* **2010**, *10*, 726–731.

(30) Fuh, Y. K.; Ye, J. C.; Chen, P. C.; Ho, H. C.; Huang, Z. M. Hybrid energy harvester consisting of piezoelectric fibers with largely enhanced 20 V for wearable and muscle-driven applications. *ACS Appl. Mater. Interfaces* **2015**, *7*, 16923–16931.

(31) Fuh, Y. K.; Chen, S. Z.; He, Z. Y. Direct-write, highly aligned chitosan-poly(ethylene oxide) nanofiber patterns for cell morphology and spreading control. *Nanoscale Res. Lett.* **2013**, *8*, 97.

(32) Fuh, Y. K.; Wu, Y. C.; He, Z. Y.; Huang, Z. M.; Hu, W. W. The control of cell orientation using biodegradable alginate fibers fabricated by near-field electrospinning. *Mater. Sci. Eng., C* **2016**, *62*, 879–887.

(33) Brown, T. D.; Dalton, P. D.; Hutmacher, D. W. Direct writing by way of melt electrospinning. *Adv. Mater.* **2011**, *23*, S651–S657.

(34) Hochleitner, G.; Jungst, T.; Brown, T. D.; Hahn, K.; Moseke, C.; Jakob, F.; Dalton, P. D.; Groll, J. Additive manufacturing of scaffolds with sub-micron filaments via melt electrospinning writing. *Biofabrication* **2015**, *7*, 035002.

(35) Liu, Z. H.; Pan, C. T.; Yen, C. K.; Lin, L. W.; Huang, J. C.; Ke, C. A. Crystallization and mechanical behavior of the ferroelectric polymer nonwoven fiber fabrics for highly durable wearable sensor applications. *Appl. Surf. Sci.* **2015**, *346*, 291–301.

(36) Shen, C.; Wang, C. P.; Sanghadasa, M.; Lin, L. Direct-write polymeric strain sensors with arbitrary contours on flexible substrates. *2016 IEEE 29th International Conference on Micro Electro Mechanical Systems (MEMS)*; 2016; pp 869–872.

(37) Wang, X.; Zheng, G. F.; He, G. Q.; Wei, J.; Liu, H. Y.; Lin, Y. H.; Zheng, J. Y.; Sun, D. H. Electrohydrodynamic direct-writing ZnO nanofibers for device applications. *Mater. Lett.* **2013**, *109*, 58–61.

(38) Zheng, G. F.; Pei, Y. B.; Wang, X.; Zheng, J. Y.; Sun, D. H. Electrohydrodynamic direct-writing of conductor-insulator-conductor multi-layer interconnection. *Chin. Phys. B* **2014**, *23*, 066102.

(39) Wang, X.; Zheng, G. F.; Xu, L.; Cheng, W.; Xu, B. L.; Huang, Y. F.; Sun, D. H. Fabrication of nanochannels via near-field electrospinning. *Appl. Phys. A: Mater. Sci. Process.* **2012**, *108*, 825–828.

(40) Lee, S. H.; Limkraisiri, K.; Gao, Y.; Chang, C.; Lin, L. W. Chip-to-chip fluidic connectors via near-field electrospinning. In *Proceedings of the IEEE Twentieth Annual International Conference on Micro Electro Mechanical Systems, Vols 1 and 2*; 2007; pp 252–255.

(41) Reneker, D. H.; Yarin, A. L. Electrospinning jets and polymer nanofibers. *Polymer* **2008**, *49*, 2387–2425.

(42) Reneker, D. H.; Yarin, A. L.; Fong, H.; Koombhongse, S. Bending instability of electrically charged liquid jets of polymer solutions in electrospinning. *J. Appl. Phys.* **2000**, *87*, 4531–4547.

(43) Baumgarten, P. K. Electrostatic spinning of acrylic microfibers. *J. Colloid Interface Sci.* **1971**, *36*, 71–79.

(44) Zheng, G.; Li, W.; Wang, X.; Wang, H.; Sun, D.; Lin, L. Experiment and simulation of coiled nanofiber deposition behavior from near-field electrospinning. *2010 5th IEEE International Conference on Nano/Micro Engineered and Molecular Systems (NEMS 2010)* **2010**, 284–288.

(45) Zheng, G. F.; Li, W. W.; Wang, X.; Wu, D. Z.; Sun, D. H.; Lin, L. W. Precision deposition of a nanofibre by near-field electrospinning. *J. Phys. D: Appl. Phys.* **2010**, *43*, 415501.

(46) Chang, C.; Limkraisiri, K.; Lin, L. Continuous near-field electrospinning for large area deposition of orderly nanofiber patterns. *Appl. Phys. Lett.* **2008**, *93*, 123111.

(47) Bisht, G. S.; Canton, G.; Mirsepassi, A.; Kulinsky, L.; Oh, S.; Dunn-Rankin, D.; Madou, M. J. Controlled continuous patterning of polymeric nanofibers on three-dimensional substrates using low-voltage near-field electrospinning. *Nano Lett.* **2011**, *11*, 1831–1837.

(48) Parajuli, D.; Koomsap, P.; Parkhi, A. A.; Supaphol, P. Experimental investigation on process parameters of near-field deposition of electrospinning-based rapid prototyping. *Virtual and Physical Prototyping* **2016**, *11*, 193–207.

(49) Zhu, Z. M.; Chen, X. D.; Huang, S. N.; Fang, F. Y.; Peng, D. Y.; Zeng, J.; Du, Z. F.; Wang, H. Solution concentration affected wavy fibers fabrication via auxiliary electrodes in near-field electrospinning. *Key Eng. Mater.* **2016**, *679*, 23–26.

(50) Zheng, J.; Long, Y. Z.; Sun, B.; Zhang, Z. H.; Shao, F.; Zhang, H. D.; Zhang, Z. M.; Huang, J. Y. Polymer nanofibers prepared by low-voltage near-field electrospinning. *Chin. Phys. B* **2012**, *21*, 048102.

(51) Katta, P.; Alessandro, M.; Ramsier, R. D.; Chase, G. G. Continuous electrospinning of aligned polymer nanofibers onto a wire drum collector. *Nano Lett.* **2004**, *4*, 2215–2218.

(52) Kameoka, J.; Orth, R.; Yang, Y. N.; Czaplewski, D.; Mathers, R.; Coates, G. W.; Craighead, H. G. A scanning tip electrospinning source for deposition of oriented nanofibers. *Nanotechnology* **2003**, *14*, 1124–1129.

(53) Wu, Y.; Johannes, M. S.; Clark, R. L. AFM-based voltage assisted nanoelectrospinning. *Mater. Lett.* **2008**, *62*, 699–702.



- (54) Lei, T. P.; Lu, X. Z.; Yang, F. Fabrication of various micro/nano structures by modified near-field electrospinning. *AIP Adv.* **2015**, *5*, 041301.
- (55) Obukhov, S. P.; Rubinstein, M.; Colby, R. H. Network modulus and superelasticity. *Macromolecules* **1994**, *27*, 3191–3198.
- (56) Fong, H.; Chun, I.; Reneker, D. H. Beaded nanofibers formed during electrospinning. *Polymer* **1999**, *40*, 4585–4592.
- (57) Shenoy, S. L.; Bates, W. D.; Frisch, H. L.; Wnek, G. E. Role of chain entanglements on fiber formation during electrospinning of polymer solutions: good solvent, non-specific polymer–polymer interaction limit. *Polymer* **2005**, *46*, 3372–3384.
- (58) Feng, J. J. Stretching of a straight electrically charged viscoelastic jet. *J. Non-Newtonian Fluid Mech.* **2003**, *116*, 55–70.
- (59) Hochleitner, G.; Hummer, J. F.; Luxenhofer, R.; Groll, J. High definition fibrous poly (2-ethyl-2-oxazoline) scaffolds through melt electrospinning writing. *Polymer* **2014**, *55*, S017–S023.
- (60) Brown, T. D.; Edin, F.; Detta, N.; Skelton, A. D.; Huttmacher, D. W.; Dalton, P. D. Melt electrospinning of poly( $\epsilon$ -caprolactone) scaffolds: Phenomenological observations associated with collection and direct writing. *Mater. Sci. Eng., C* **2014**, *45*, 698–708.
- (61) Brown, T. D.; Slotosch, A.; Thibaudeau, L.; Taubenberger, A.; Loessner, D.; Vaquette, C.; Dalton, P. D.; Huttmacher, D. W. Design and fabrication of tubular scaffolds via direct writing in a melt electrospinning mode. *Biointerphases* **2012**, *7*, 13.
- (62) Dalton, P. D.; Vaquette, C.; Farrugia, B. L.; Dargaville, T. R.; Brown, T. D.; Huttmacher, D. W. Electrospinning and additive manufacturing: converging technologies. *Biomater. Sci.* **2013**, *1*, 171–185.
- (63) Kruth, J. P.; Leu, M. C.; Nakagawa, T. Progress in additive manufacturing and rapid prototyping. *CIRP Ann.* **1998**, *47*, S25–S40.
- (64) Murr, L. E.; Gaytan, S. M.; Ramirez, D. A.; Martinez, E.; Hernandez, J.; Amato, K. N.; Shindo, P. W.; Medina, F. R.; Wicker, R. B. Metal fabrication by additive manufacturing using laser and electron beam melting technologies. *J. Mater. Sci. Technol.* **2012**, *28*, 1–14.
- (65) Hu, D. M.; Kovacevic, R. Sensing, modeling and control for laser-based additive manufacturing. *Int. J. Mach. Tool. Manu.* **2003**, *43*, 51–60.
- (66) Cumpston, B. H.; Ananthavel, S. P.; Barlow, S.; Dyer, D. L.; Ehrlich, J. E.; Erskine, L. L.; Heikal, A. A.; Kuebler, S. M.; Lee, I. Y. S.; McCord-Maughon, D.; Qin, J. Q.; Rockel, H.; Rumi, M.; Wu, X. L.; Marder, S. R.; Perry, J. W. Two-photon polymerization initiators for three-dimensional optical data storage and microfabrication. *Nature* **1999**, *398*, 51–54.
- (67) Williams, J. M.; Adewunmi, A.; Schek, R. M.; Flanagan, C. L.; Krebsbach, P. H.; Feinberg, S. E.; Hollister, S. J.; Das, S. Bone tissue engineering using polycaprolactone scaffolds fabricated via selective laser sintering. *Biomaterials* **2005**, *26*, 4817–4827.
- (68) Jacobs, P. F. *Rapid prototyping & manufacturing: fundamentals of stereolithography*; Society of Manufacturing Engineers: 1993.
- (69) Huttmacher, D. W.; Schantz, T.; Zein, I.; Ng, K. W.; Teoh, S. H.; Tan, K. C. Mechanical properties and cell cultural response of polycaprolactone scaffolds designed and fabricated via fused deposition modeling. *J. Biomed. Mater. Res.* **2001**, *55*, 203–216.
- (70) Pan, C. T.; Yang, T. L.; Chen, Y. C.; Su, C. Y.; Ju, S. P.; Hung, K. H.; Wu, I. C.; Hsieh, C. C.; Shen, S. C. Fibers and conductive films using silver nanoparticles and nanowires by near-field electrospinning process. *J. Nanomater.* **2015**, *2015*, 1–5.
- (71) Yang, T. L.; Pan, C. T.; Chen, Y. C.; Lin, L. W.; Wu, I. C.; Hung, K. H.; Lin, Y. R.; Huang, H. L.; Liu, C. F.; Mao, S. W.; Kuo, S. W. Synthesis and fabrication of silver nanowires embedded in PVP fibers by near-field electrospinning process. *Opt. Mater.* **2015**, *39*, 118–124.
- (72) Zhou, F. L.; Hubbard, P. L.; Eichhorn, S. J.; Parker, G. J. M. Jet deposition in near-field electrospinning of patterned polycaprolactone and sugar-polycaprolactone core-shell fibres. *Polymer* **2011**, *52*, 3603–3610.
- (73) Xin, Y.; Reneker, D. H. Hierarchical polystyrene patterns produced by electrospinning. *Polymer* **2012**, *53*, 4254–4261.
- (74) Fuh, Y. K.; Chen, S. Y.; Ye, J. C. Massively parallel aligned microfibers-based harvester deposited via in situ, oriented poled near-field electrospinning. *Appl. Phys. Lett.* **2013**, *103*, 033114.
- (75) Liu, Z. H.; Pan, C. T.; Lin, L. W.; Huang, J. C.; Ou, Z. Y. Direct-write PVDF nonwoven fiber fabric energy harvesters via the hollow cylindrical near-field electrospinning process. *Smart Mater. Struct.* **2014**, *23*, 025003.
- (76) Di Camillo, D.; Fasano, V.; Ruggieri, F.; Santucci, S.; Lozzi, L.; Camposeo, A.; Pisignano, D. Near-field electrospinning of light-emitting conjugated polymer nanofibers. *Nanoscale* **2013**, *5*, 11637–11642.
- (77) Zhu, Z. M.; Chen, X. D.; Du, Z. F.; Huang, S. N.; Peng, D. Y.; Zheng, J. W.; Wang, H. Fabricated wavy micro/nanofiber via auxiliary electrodes in near-field electrospinning. *Mater. Manuf. Processes* **2016**, *31*, 707–712.
- (78) Zhu, Z. M.; Chen, X. D.; Huang, S. N.; Du, Z. F.; Zeng, J.; Liao, W. Y.; Fang, F. Y.; Peng, D. Y.; Wang, H. The process of wavy fiber deposition via auxiliary electrodes in near-field electrospinning. *Appl. Phys. A: Mater. Sci. Process.* **2015**, *120*, 1435–1442.
- (79) Rinaldi, M.; Ruggieri, F.; Lozzi, L.; Santucci, S. Well-aligned TiO<sub>2</sub> nanofibers grown by near-field-electrospinning. *J. Vac. Sci. Technol. B* **2009**, *27*, 1829–1833.
- (80) Chang, J.; Lin, L. Large array electrospun PVDF nanogenerators on a flexible substrate. *2016 IEEE 29th International Conference on Micro Electro Mechanical Systems (MEMS)*; 2011; pp 747–750.
- (81) Luo, G.; Teh, K. S.; Zang, X.; Wu, D.; Wen, Z.; Lin, L. High aspect-ratio 3D microstructures via near-field electrospinning for energy storage applications. *2016 IEEE 29th International Conference on Micro Electro Mechanical Systems (MEMS)*; 2016; pp 29–32.
- (82) Hellmann, C.; Belardi, J.; Dersch, R.; Greiner, A.; Wendorff, J. H.; Bahnmüller, S. High precision deposition electrospinning of nanofibers and nanofiber nonwovens. *Polymer* **2009**, *50*, 1197–1205.
- (83) Wang, H.; Li, M. H.; Chen, X.; Zheng, J. W.; Chen, X. D.; Zhu, Z. M. Study of deposition characteristics of multi-nozzle near-field electrospinning in electric field crossover interference conditions. *AIP Adv.* **2015**, *5*, 041302.
- (84) Huang, S. N.; Chen, X. D.; Wang, Z. F.; Zeng, J.; Fang, F. Y.; Wang, H. An investigation on multi-nozzle near field electrospinning: experimentation and simulation. *Key Eng. Mater.* **2016**, *679*, 63–66.
- (85) Wang, Z. F.; Chen, X. D.; Huang, S. N.; Fang, F. Y.; Wang, H. Research on deposition characteristics of the double-nozzle in near-field electrospinning. *Key Eng. Mater.* **2016**, *679*, 59–62.
- (86) Sun, B.; Long, Y. Z.; Liu, S. L.; Huang, Y. Y.; Ma, J.; Zhang, H. D.; Shen, G. Z.; Xu, S. Fabrication of curled conducting polymer microfibrous arrays via a novel electrospinning method for stretchable strain sensors. *Nanoscale* **2013**, *5*, 7041–7045.
- (87) Motojima, S.; Chen, Q. Q. Three-dimensional growth mechanism of cosmo-mimetic carbon microcoils obtained by chemical vapor deposition. *J. Appl. Phys.* **1999**, *85*, 3919–3921.
- (88) Kong, X. Y.; Wang, Z. L. Spontaneous polarization-induced nanohelices, nanosprings, and nanorings of piezoelectric nanobelts. *Nano Lett.* **2003**, *3*, 1625–1631.
- (89) Huang, Y. A.; Bu, N. B.; Duan, Y. Q.; Pan, Y. Q.; Liu, H. M.; Yin, Z. P.; Xiong, Y. L. Electrohydrodynamic direct-writing. *Nanoscale* **2013**, *5*, 12007–12017.
- (90) Huang, Y. P. Review of long period fiber gratings written by CO<sub>2</sub> laser. *J. Appl. Phys.* **2010**, *108*, 081101.
- (91) Martinez-Prieto, N.; Abecassis, M.; Xu, J.; Guo, P.; Cao, J.; Ehmman, K. F. Feasibility of fiber-deposition control by secondary electric fields in near-field electrospinning. *Journal of Micro and Nano-Manufacturing* **2015**, *3*, 041005–041005.
- (92) Lu, X.; McElroy, M. B.; Kiviluoma, J. Global potential for wind-generated electricity. *Proc. Natl. Acad. Sci. U. S. A.* **2009**, *106*, 10933–10938.
- (93) Scruggs, J.; Jacob, P. Harvesting ocean wave energy. *Science* **2009**, *323*, 1176–1178.
- (94) Paradiso, J. A.; Starner, T. Energy scavenging for mobile and wireless electronics. *IEEE Pervas. Comput.* **2005**, *4*, 18–27.
- (95) Donelan, J. M.; Li, Q.; Naing, V.; Hoffer, J. A.; Weber, D. J.; Kuo, A. D. Biomechanical energy harvesting: Generating electricity during walking with minimal user effort. *Science* **2008**, *319*, 807–810.
- (96) Wang, Z. L.; Song, J. H. Piezoelectric nanogenerators based on zinc oxide nanowire arrays. *Science* **2006**, *312*, 242–246.

- (97) Zhu, G. A.; Yang, R. S.; Wang, S. H.; Wang, Z. L. Flexible high-output nanogenerator based on lateral ZnO nanowire array. *Nano Lett.* **2010**, *10*, 3151–3155.
- (98) Baji, A.; Mai, Y. W.; Li, Q.; Liu, Y. Electrospinning induced ferroelectricity in poly(vinylidene fluoride) fibers. *Nanoscale* **2011**, *3*, 3068–3071.
- (99) Hansen, B. J.; Liu, Y.; Yang, R. S.; Wang, Z. L. Hybrid nanogenerator for concurrently harvesting biomechanical and biochemical energy. *ACS Nano* **2010**, *4*, 3647–3652.
- (100) Ma, S.; Sun, Q.; Su, Y.; Chen, R.; Wang, L. Y. Experimental investigation of piezoelectricity of near field electrospun PVDF nanofibers. *TELKOMNIKA (Telecommunication Computing Electronics and Control)* **2016**, *14*, 145–151.
- (101) Fuh, Y. K.; Wang, B. S. Near field sequentially electrospun three-dimensional piezoelectric fibers arrays for self-powered sensors of human gesture recognition. *Nano Energy* **2016**, *30*, 677–683.
- (102) Pan, C. T.; Yen, C. K.; Wu, H. C.; Lin, L. W.; Lu, Y. S.; Huang, J. C. C.; Kuo, S. W. Significant piezoelectric and energy harvesting enhancement of poly(vinylidene fluoride)/polypeptide fiber composites prepared through near-field electrospinning. *J. Mater. Chem. A* **2015**, *3*, 6835–6843.
- (103) Nam, Y. S.; Park, T. G. Porous biodegradable polymeric scaffolds prepared by thermally induced phase separation. *J. Biomed. Mater. Res.* **1999**, *47*, 8–17.
- (104) Chirila, T. V.; Higgins, B.; Dalton, P. D. The effect of synthesis conditions on the properties of poly(2-hydroxyethyl methacrylate) sponges. *Cell. Polym.* **1998**, *17*, 141–162.
- (105) Hollister, S. H. Porous scaffold design for tissue engineering. *Nat. Mater.* **2005**, *4*, 518–524.
- (106) Holy, C. E.; Dang, S. M.; Davies, J. E.; Shoichet, M. S. In vitro degradation of a novel poly(lactide-co-glycolide) 75/25 foam. *Biomaterials* **1999**, *20*, 1177–1185.
- (107) Kim, D. D.; Takeno, M. M.; Ratner, B. D.; Horbett, T. A. Glow discharge plasma deposition (GDPD) technique for the local controlled delivery of hirudin from biomaterials. *Pharm. Res.* **1998**, *15*, 783–786.
- (108) Yoshimoto, H.; Shin, Y. M.; Terai, H.; Vacanti, J. P. A biodegradable nanofiber scaffold by electrospinning and its potential for bone tissue engineering. *Biomaterials* **2003**, *24*, 2077–2082.
- (109) Schneider, O. D.; Lohrer, S.; Brunner, T. J.; Schmidlin, P.; Stark, W. J. Flexible, silver containing nanocomposites for the repair of bone defects: antimicrobial effect against *E. coli* infection and comparison to tetracycline containing scaffolds. *J. Mater. Chem.* **2008**, *18*, 2679.
- (110) Laurencin, C. T.; Ambrosio, A. M. A.; Borden, M. D.; Cooper, J. J. A. Tissue engineering: orthopedic applications. Annual review of biomedical engineering. *Annu. Rev. Biomed. Eng.* **1999**, *1*, 19–46.
- (111) Rowley, J. A.; Madlambayan, G.; Mooney, D. J. Alginate hydrogels as synthetic extracellular matrix materials. *Biomaterials* **1999**, *20*, 45–53.
- (112) Liu, N.; Fang, G.; Wan, J.; Zhou, H.; Long, H.; Zhao, X. Electrospun PEDOT: PSS–PVA nanofiber based ultrahigh-strain sensors with controllable electrical conductivity. *J. Mater. Chem.* **2011**, *21*, 18962.
- (113) Wang, X. W.; Gu, Y.; Xiong, Z. P.; Cui, Z.; Zhang, T. Silk-molded flexible, ultrasensitive, and highly stable electronic skin for monitoring human physiological signals. *Adv. Mater.* **2014**, *26*, 1336–1342.
- (114) Kim, N. W.; Lee, S. J.; Lee, B. G.; Lee, J. J. Vision based laser pointer interaction for flexible screens. *Human-Computer Interaction. Interaction Platforms and Techniques*; International Conference on Human-Computer Interaction; Springer: Berlin and Heidelberg, Germany, 2007; pp 845–853.
- (115) Ko, H.; Lee, J.; Kim, Y.; Lee, B.; Jung, C. H.; Choi, J. H.; Kwon, O. S.; Shin, K. Active digital microfluidic paper chips with inkjet-printed patterned electrodes. *Adv. Mater.* **2014**, *26*, 2335–2340.
- (116) Gullapalli, H.; Vemuru, V. S. M.; Kumar, A.; Botello-Mendez, A.; Vajtai, R.; Terrones, M.; Nagarajaiah, S.; Ajayan, P. M. Flexible piezoelectric ZnO–paper nanocomposite strain sensor. *Small* **2010**, *6*, 1641–1646.
- (117) Youn, D. H.; Yu, Y. J.; Choi, J. S.; Park, N. M.; Yun, S. J.; Lee, I.; Kim, G. H. Transparent conducting films of silver hybrid films formed by near-field electrospinning. *Mater. Lett.* **2016**, *185*, 139–142.
- (118) Li, T.; Hu, W.; Zhu, D. Nanogap electrodes. *Adv. Mater.* **2010**, *22*, 286–300.
- (119) Liu, X.; Gu, L.; Zhang, Q.; Wu, J.; Long, Y. Z.; Fan, Z. All-printable band-edge modulated ZnO nanowire photodetectors with ultra-high detectivity. *Nat. Commun.* **2014**, *5*, 4007.
- (120) Friend, R. H.; Gymer, R. W.; Holmes, A. B.; Burroughes, J. H.; Marks, R. N.; Taliani, C.; Bradley, D. D. C.; Dos Santos, D. A.; Bredas, J. L.; Logdlund, M.; Salaneck, W. R. Electroluminescence in conjugated polymers. *Nature* **1999**, *397*, 121–128.
- (121) Facchetti, A.  $\pi$ -conjugated polymers for organic electronics and photovoltaic cell applications. *Chem. Mater.* **2011**, *23*, 733–758.
- (122) Alam, M. M.; Jenekhe, S. A. Polybenzobisazoles are efficient electron transport materials for improving the performance and stability of polymer light-emitting diodes. *Chem. Mater.* **2002**, *14*, 4775–4780.
- (123) Li, D.; Babel, A.; Jenekhe, S. A.; Xia, Y. N. Nanofibers of conjugated polymers prepared by electrospinning with a two-capillary spinneret. *Adv. Mater.* **2004**, *16*, 2062–2066.
- (124) Ishii, Y.; Sakai, H.; Murata, H. A new electrospinning method to control the number and a diameter of uniaxially aligned polymer fibers. *Mater. Lett.* **2008**, *62*, 3370–3372.
- (125) Di Benedetto, F.; Camposeo, A.; Pagliara, S.; Mele, E.; Persano, L.; Stabile, R.; Cingolani, R.; Pisignano, D. Patterning of light-emitting conjugated polymer nanofibers. *Nat. Nanotechnol.* **2008**, *3*, 614–619.
- (126) Camposeo, A.; Persano, L.; Pisignano, D. Light-emitting electrospun nanofibers for nanophotonics and optoelectronics. *Macromol. Mater. Eng.* **2013**, *298*, 487–503.
- (127) Hochleitner, G.; Youssef, A.; Hrynevich, A.; Haigh, J.; Junst, T.; Groll, J.; Dalton, P. D. Fibre pulsing during melt electrospinning writing. *Biomaterials* **2016**, *17*, 159–171.
- (128) Shen, C. W.; Wang, C. P. Flexible micro-supercapacitors prepared using direct-write nanofiber. *RSC Adv.* **2017**, *7*, 11724–11731.